THE STUDY OF THERMODYNAMICS PROPERTIES OF CARBON-BASED MATERIAL USING MOLECULAR DYNAMICS SIMULATION

by

MIN TJUN KIT
(1061106195)

Session 2010/2011

B.Eng. (Hons) Electronics Majoring in Nanotechnology

The project report is prepared for
Faculty of Engineering
Multimedia University
in partial fulfillment for
Bachelor of Engineering

FACULTY OF ENGINEERING
MULTIMEDIA UNIVERSITY
MAY 2011

DECLARATION

I hereby declare that this work has been done by myself and no portion of the work contained in this report has been submitted in support of any application for any other degree or qualification of this or any other university or institute of learning.

I also declare that pursuant to the provisions of the Copyright Act 1987, I have not engaged in any unauthorised act of copying or reproducing or attempt to copy / reproduce or cause to copy / reproduce or permit the copying / reproducing or the sharing and / or downloading of any copyrighted material or an attempt to do so whether by use of the University's facilities or outside networks / facilities whether in hard copy or soft copy format, of any material protected under the provisions of sections 3 and 7 of the Act whether for payment or otherwise save as specifically provided for therein. This shall include but not be limited to any lecture notes, course packs, thesis, text books, exam questions, any works of authorship fixed in any tangible medium of expression whether provided by the University or otherwise.

I hereby further declare that in the event of any infringement of the provisions of the Act whether knowingly or unknowingly the University shall not be liable for the same in any manner whatsoever and undertake to indemnify and keep indemnified the University against all such claims and actions.

Signature: _____

Name : MIN TJUN KIT

Student ID : 1061106195

Date : 18th April 2011

To Dr. Yoon Tiem Leong for constant encouragement and support

ACKNOWLEDGEMENT

No product is ever a result of the hard work of just one person. I believe that there are many who deserve a proper acknowledgement for this beautiful piece of work.

First of all special thanks goes to my final year project supervisor Mr. Choo Kan Yeep for the constant guidance and directions given to me from the first day I chose to do the project. I would like extend my sincere gratitude towards Ms. Lau Pei Ling. for her valuable time in evaluating the project.

Next thanks to Dr. Yoon Tiem Leong and Dr. Lim Thong Leng for allowing me access to USM Comsics server to do my project. And also thanks to their constant support and guidance.

Finally I would like to thank all those who contributed, both directly and indirectly, towards the successful completion of my final year project.

ABSTRACT

The main objective of the final year project is to determine the physical properties of carbon nanostructures such as carbon nanotube and graphene sheets and how the properties evolve when the structure transforms from 2D to 3D (bulk material). Molecular dynamics simulations with AIREBO potential is used to study the thermodynamic properties of the carbon nanostructure and is performed using LAMMPS simulation code. The simulations involve the evolution of atoms or molecules at finite temperature field. The single wall nanotube is being investigated for its thermodynamic properties such as thermal conductivity, phase transition and heat capacity. Next, the thermodynamic properties of single layer graphene to multiple layers of graphe (graphite) were also being investigated. The simulation results indicate that the thermodynamic properties of graphene will change to graphite when seveb layers of graphene are formed together.

TABLE OF CONTENTS

LIST OF TABLES

LIST OF FIGURES

CHAPTER 1

INTRODUCTION

The nanotechnology today has played a very large role on the properties of the material in nanoscale. The bulk of the work so far has been either approach experimentally or theoretically and there are lacks of agreement of results in various groups. So it is vital to back to fundamental study in order to fully understand a phenomenon. Molecular modeling is one of a wise approach to observe the thermodynamics properties in nanoscale. Thermodynamics properties can be several kinds such as thermal conductivity, melting temperature, diffusion coefficient and heat capacity. Our aim is to characterize these properties using molecular dynamics. It has several applications such as thermal management of electronics device (thermo-electronics) [1], nanofabrication techniques [2], as well as efficient kinetic energy transfer of nanoscale.

1.1 Motivation

Thermal transport at nanoscale is now growing interest in research community. The most significant study is on thermal conductivity of a material. It defines how fast can heat transport from a point to another. Molecular dynamics has offer a great tool to study the thermal conductivity of a materials.

Others properties such as phase transition, diffusivity and heat capacity are also can be investigated using molecular simulation. Heat capacity is very interesting to study from solid at constant temperature. The behavior is comparable with harmonic solid or ideal gas. The heat capacity is determined from fluctuations of energy. Note that phase transition is quite difficult to locate, as there has a strong hysteresis in physical quantity.

The information of phase transition will provide us information of melting/solidification or evaporation of a material. At phase change there is sudden increase of potential energy and volume of a material. Different phase of material will have different applications. Material with high diffusivity can rapidly adjust their temperature correlated with their surrounding because they conduct heat efficiently and generally do not need much energy from surrounding to reach thermal equilibrium. This information is very important in high speed computing system, high speed lubrication process and fibre manufacturing process.

Molecular dynamics simulation has greatly enhance the research in nanoscience. It saves cost, resources and time that are required by experiment. Molecular simulation can used to study many unanswered question there is very hard to perform by experiment such as study the properties of nanoporous materials because the process involve molecular forces. It is not so computationally intensive compare to Density Functional Theory or Quantum Monte Carlo while still provides quite accurate result. It is also suitable to study static and dynamics system. Hence, Molecular Dynamics has chosen as preferred method.

However, different simulation and experiment may give to result ambiguity. So the result of the simulation will compare among each others may provide some information of the system.

1.2 Objective

The major aim of the project is to characterise the thermodynamic properties of carbon nanostructures through molecular dynamics simulation. The thermodynamics properties of CNT, graphene and multi layers of graphene are simulated. The effect of carbon layers on properties of graphene is determined.

1.3 Organisation of Thesis

Chapter 1 briefly describes molecular dynamics simulation approach on determination of thermodynamic properties of carbon nanostructures. Besides that, the objectives and motivations of the project are described in this chapter. The basic information of carbon nanostructure, molecular dynamics simulation and thermodynamic properties are discussed in Chapter 2. This includes various thermodynamic properties such as thermal conductivity, diffusion coefficient, phase transition and specific heat capacity. Chapter 3 describes the simulation methodology regarding computational calculation of thermodynamic properties of carbon nanostructures using LAMMPS. In Chapter 4, the results and discussions are presented here in comparison with experimental results. The summary of the final year project and recommendation is discussed in Chapter 5.

CHAPTER 2

BACKGROUND THEORY

2.1 Carbon Nanostructures

Carbon nanostructures such as carbon nanotube, graphene and graphite are graphitic structures (sp^2-hybridized) made of carbon and have characteristic dimensions of magnitude order of nanometer. Today, they have attracted worldwide attention and have multiple applications. Carbon nanotubes are graphene sheet rolled into tube size with diameter of nanometers. Carbon nanotubes (CNT) possess outstanding physical properties compare to bulk carbon materials. Their metallic/semiconducting behavior and mechanical properties are very interesting topic to study compared to bulk carbon material [3]. Carbon nanotubes usually grown on transitional metallic surface by using suitable catalyst. 2D graphene sheet can be synthesis through "scotch tape cleaving" of 3D graphite until it reaches single layer of carbon atoms [4]. The graphene has enhanced strength and thermal properties compared to CNT [5][6].

There are three types of carbon nanotubes. Specifically armchair, zigzag and chiral that has been shown in Fig. 2.1 which is depending of their chirality which means the amount of "twist" or orientation in the tube.

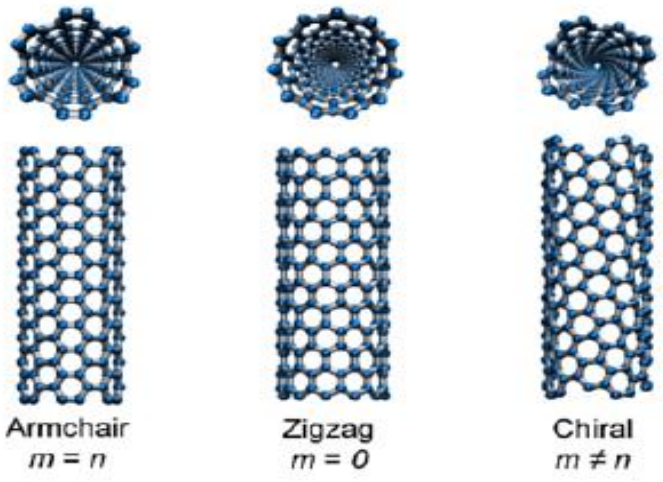

Figure 2.1: Types of carbon nanotubes and its chirality.

A CNT is characterized in term of tube chirality by its chiral vector, the chiral vector, *C*, can be written as combination of lattice basis vector as shown in Fig. 2.2:

$$C = na_1 + ma_2 \tag{2.1}$$

The angle, θ, respect to the zigzag axis, the integers (*n*, *m*) are the number of steps along the ziz-zag carbon bonds of the hexagonal lattice and a_1 and a_2 are unit vectors. The two limiting cases exist where the chiral angle is at 0° and 30°. These limiting cases are referred to as ziz-zag (0°) and armchair (30°) based on the geometry of the carbon bonds around the circumference of the nanotube.

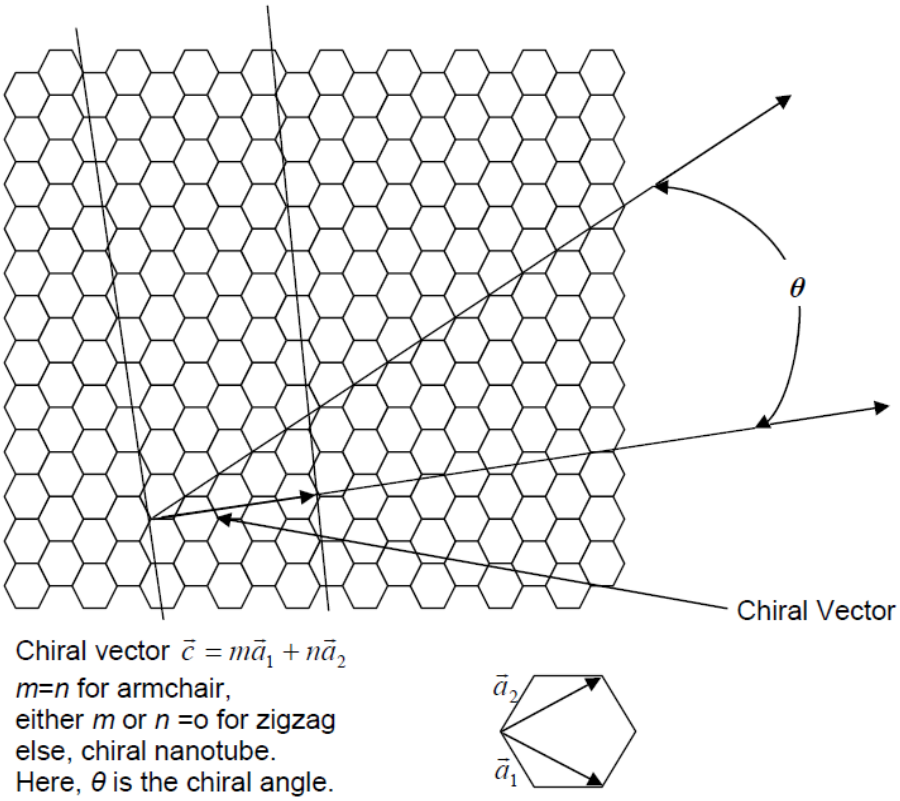

Figure 2.2: The nanotube that can formed by its chiral angle [6].

The length of chiral vector will define the circumference of the CNT. Thus, the diameter, d of CNT is defined as:

$$d = \frac{C}{\pi} \tag{2.2}$$

$$= a\sqrt{n^2 + mn + m^2} \tag{2.3}$$

Here, a = 2.49 Angstrom is the lattice constant of the graphene honeycomb lattice. There are two types of carbon nanotube as shown in Fig 2.3, which is single-wall nanotube (SWNT), which is consisting of single layer of carbon. It has greater tendency to align into ordered bundles and often used to test the theory of nanotube. Another type is multi-wall nanotube (MWNT), which is consisting of two or more layers of carbon, and it tends to form unordered clump. However, MWNT is easier to synthesis.

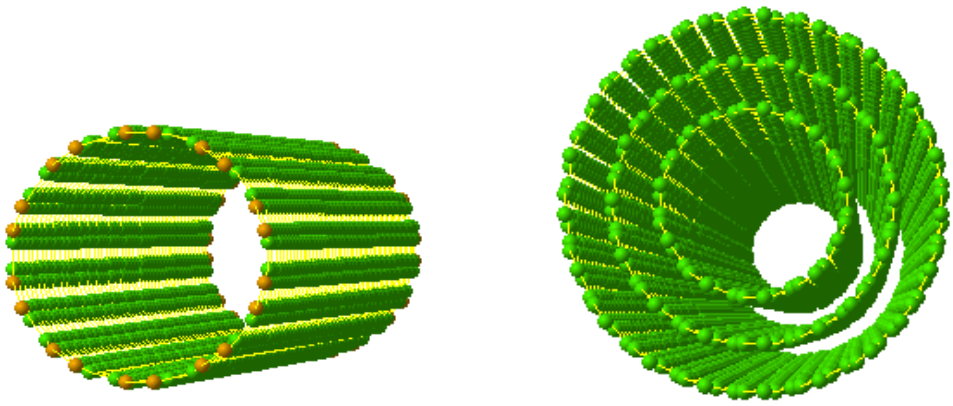

Figure 2.3: Single wall nanotube (left) and multi wall nanotube (right)[6].

Various carbon nanostructures are shown in Fig. 2.4. Graphene is a flat monolayer of carbon atoms tightly pack in 2-dimensional honeycomb lattice [7]. The bond length between carbon chains is approximately 0.142 nm. The Nobel Prize of Physics 2010 was awarded to Andre Geim and Konstantin Novoselov for ground breaking experiment regarding the 2D material graphene.

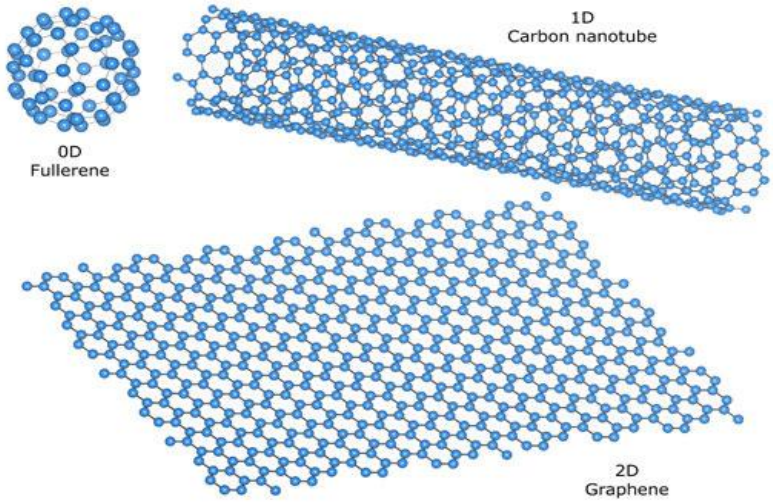

Figure 2.4: Low-dimensional carbon allotropes: fullerene (0D), carbon nanotube (1D) and graphene (2D) [7].

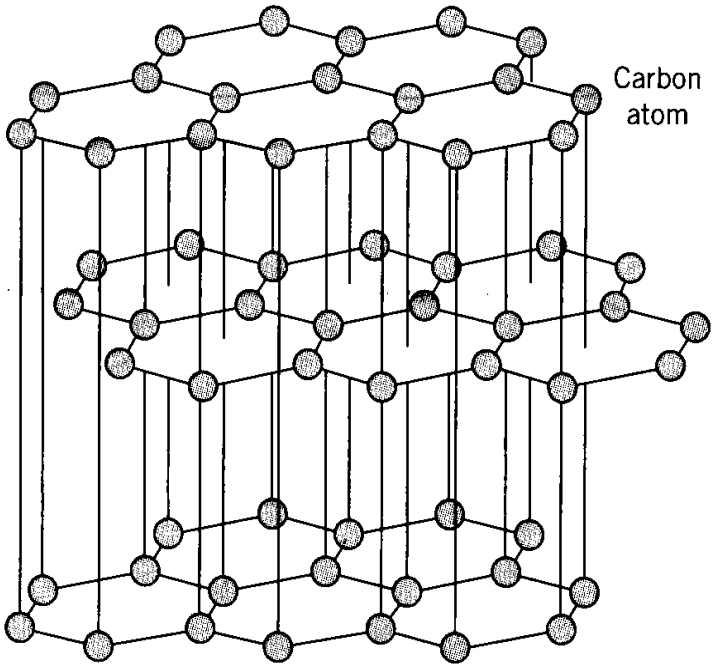

Figure 2.5: Structure of Graphite [8].

The material is generally greyish-black, opaque and has a lustrous black sheen. It is unique in that it has properties of both a metal and a non-metal. It is flexible but not elastic, has a high thermal and electrical conductivity, and has high refractor index and chemically inert. When the graphene sheets stack, it will form graphite as shown in Fig. 2.5. The crystalline or "flake" form of graphite consists of many graphene sheets stacked together. The high degree of anisotropy in graphite results from the two types of bonding acting in different crystallographic directions [8]. The spacing between the carbon layers are usually 0.335 nm and 1mm thick bulk graphite consist of 3 million layers. Graphite tends to easy to synthesis and manipulates than graphene sheet and has a low adsorption of X-rays and neutrons making it a particularly useful material in nuclear applications.

2.2 Molecular Dynamics Simulation

Molecular dynamics simulation is used to compute the motions, trajectories and velocities of particles (atom, molecule, ion or compound) in different phases [9]. It is effectively predict the physical properties of material. In the molecular dynamics simulation, the atoms or molecules are allowed to interact with each other at finite temperature for a period of time. The interactive forces or so called force field will be implemented into the system for the atom or molecule to evolve. The forces that govern the motion of atom derive from Newton Second law ($F = ma$) and classical mechanics. The evolution of the system is solved using equation of motions of all particles in the system.

$$\frac{dr_i}{dt} = v_i \tag{2.4}$$

$$\frac{d}{dt}(m_i v_i) = F_i = -\nabla_i V = -\nabla_i [\sum_j V_2(r_i, r_j) + \sum_{j,k} V_3(r_i, r_j, r_k) + \cdots] \tag{2.5}$$

Where *i* denotes as particle in the system, V is the interactive potential between particles in the system, r_i is the position of the particles in the system and v_i is the velocity of the system. The initial condition of any molecular dynamics simulation must have a well-defined initial positions and velocities of particles and provide accurate force field to derive the force among particles. The basic molecular dynamics algorithm is shown in the below flow chart in Fig. 2.6.

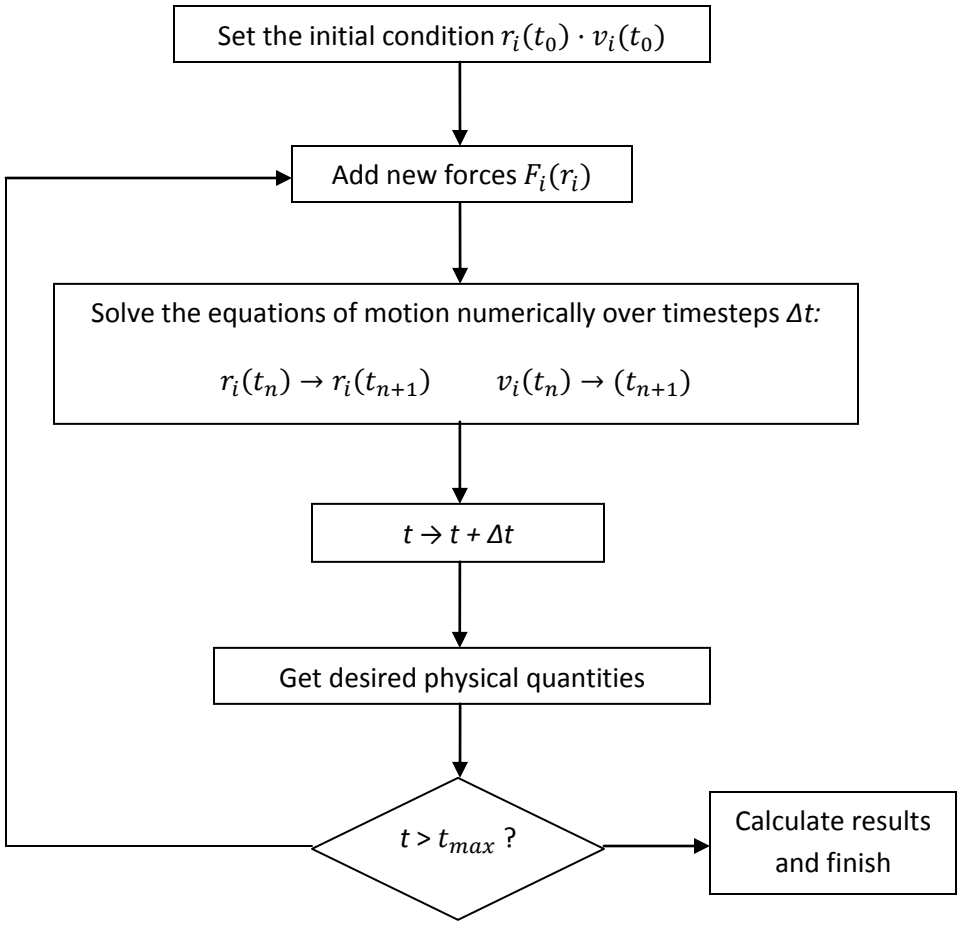

Figure 2.6: The flow chart of the molecular dynamics [9].

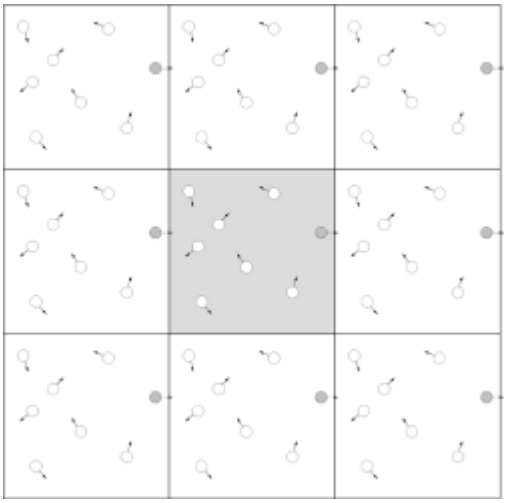

Figure 2.7: Periodic boundary condition of molecular dynamics. Each particle not only interacts with every other particle in the system but also with all other particles in the copies of the system. The arrows from the particles point to nearest copy of other particles in the system [9].

The simulated atom or molecules are placed in a simulation box with periodic boundary condition as shown in Fig. 2.7. This trick essentially eliminates the boundary effect at the edge. It is an artificial simulation of infinite volume. Because of the periodic boundary condition, we can artificially create a bulk or superlattice by replicating the simulation box because the atom will still retain is interaction with their neighboring atom.

The implementation of the molecular dynamics simulation is performed using LAMMPS (Large-scale Atomic/Molecular Massively Parallel Simulator) software. The software was run on Rocks Cluster and Comsics nodes. It requires input scripts to be written and it will be executed according to the sequence has been assigned. The detail list of how input script is written will be specified in Appendix.

Molecular dynamics simulation is compared with other simulation method as shown in Fig. 2.8. For example the comparison with Monte Carlo simulation. They have

their own advantages against each other depending on the system that has to be simulated. Molecular dynamics constantly tracking and updating the velocities and positions of particles by solving the equation of motion, while Monte Carlo simulation is a stochastic method that sampling a set of random movement or position of particles, accepting or rejecting it based on a guiding function provided. This means Monte Carlo method is usually time dependant. In other words, Monte Carlo consumes less computational resources compared to molecular dynamics simulation. However if there is too many rejected stochastic motion (highly sophisticated system), longer computational time is required. So, Monte Carlo simulation is more suitable for small to moderate system because in a highly complex system, a good sampling skill is required to reduce computational cost (mostly trial and error). Another advantage of molecular dynamics simulation over Monte Carlo simulation is molecular dynamics is designed for dynamics system (e.g. properties related to increase of temperature) which conventional Monte Carlo simulation unable to perform. However, molecular dynamics is incapable of handling the lost of atom inside the simulation box during a run. So the number of the particle inside a simulation box has to be constant. This problem does not occur for Monte Carlo simulation. Grand Canonical Monte Carlo (GCMC) can handle the variable numbers of particles.

Another atomistic modeling so called Density Functional Theory is also widely used. It is a quantum mechanical method that solved wave function of Schrodinger equation. This provides great accuracy as compared with molecular dynamics which is only using classical Newtonian approach. However, the major drawback of density functional theory is can only provide ground state information (at 0 K temperatures) which is static. Another problem is solving the Schrodinger equation is very computational intensive, if the simulation is performed more than ten atoms, the computer might jammed. So, molecular dynamics simulation is preferred.

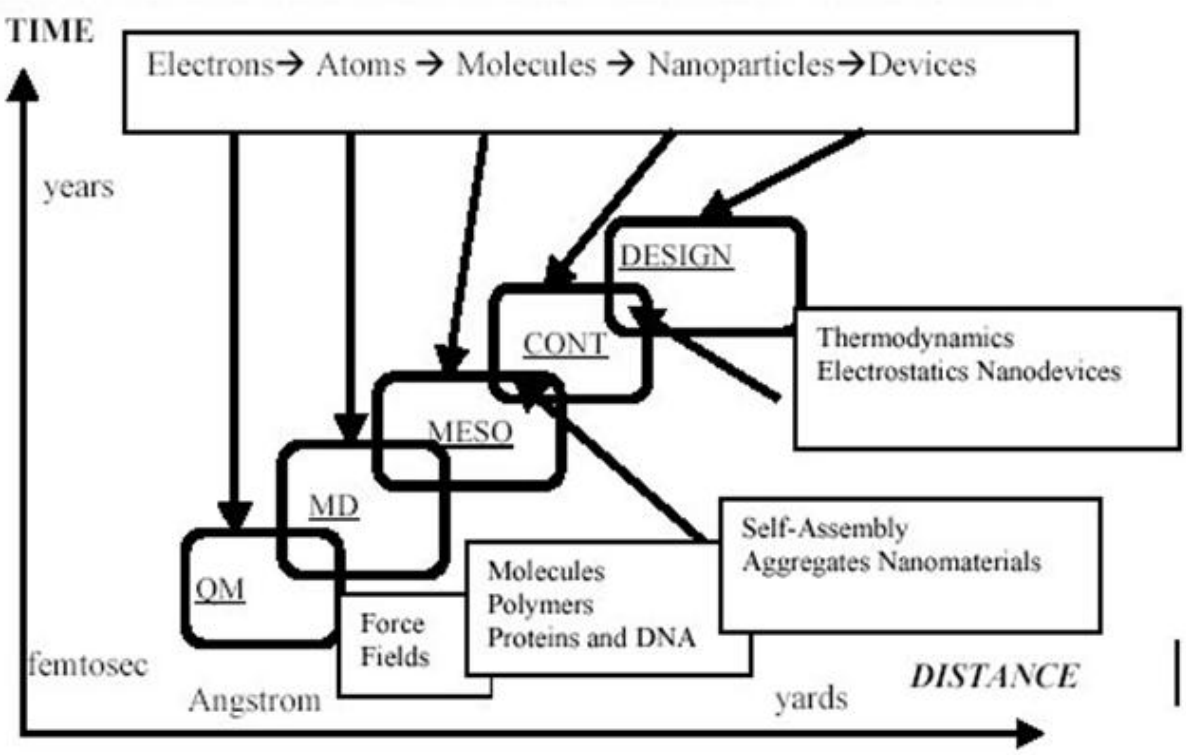

Figure 2.8: Hierarchy of computational nanoscience and molecular engineering [9].

2.2.1 Initialization

To initialize the quantity of the system to begin the simulation. The initial configuration of the system can be determined through experimentally or literature. The dimensionality, boundary condition (periodic or fixed), atomic positions, timesteps, unit cells and simulation box size are those parameters that can be tuned.

2.2.2 Force Field Implementation

Interactive potential needs to be defined in a system. A suitable empirical potential has been chosen as a function of time. The simplest and most common potential is Lennard-Jones potential with Coulombic term as shown in Fig. 2.9 [10].

$$V_{ij} = 4\varepsilon_{ij}[(\frac{\sigma_{ij}}{r_{ij}})^{12} - (\frac{\sigma_{ij}}{r_{ij}})^{6}] + \frac{q_1 q_2}{r^2} \quad (2.6)$$

V_{ij} denotes the interacting potential between particle *i* and *j*. ε and σ is the Lennard-Jones coefficient of the system, *r* is the distance between pair atoms and *q* denotes at charge of the atoms. The potential parameters like the coefficient and charge usually acquire through literature.

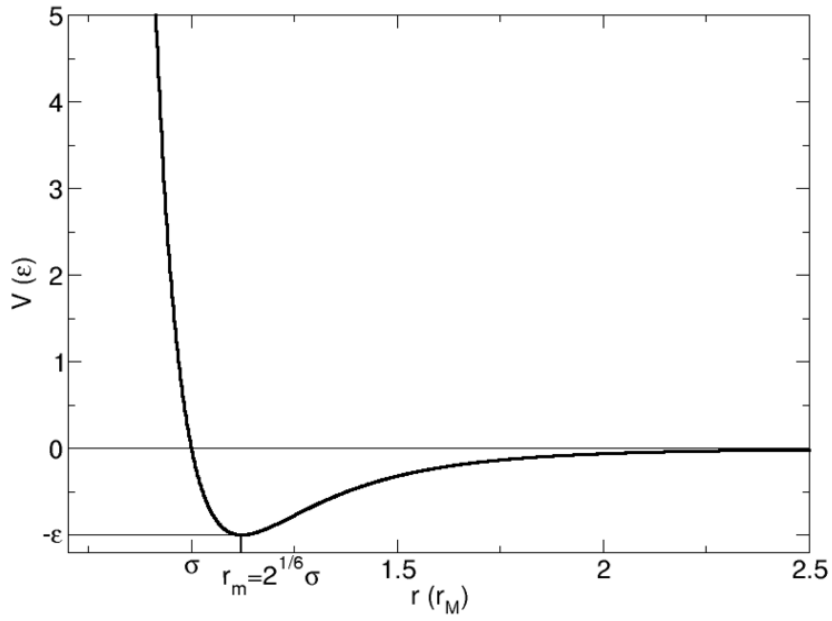

Figure 2.9: Lennard-Jones potential as function of $V(\varepsilon)$ versus r of a pair of argon atom. The atoms are at equilibrium repulsion at the radius $r_m = 2^{\frac{1}{6}}\sigma$ [10].

When two atoms *i* and *j* interact with each other under the interatomic potential on finite temperature, a force constant can be derived from the potential gradient. The forces of an atom due to other atoms in the system can be determined, thus, acceleration of the atoms can be pinpointed at any instance. Performing integration on the acceleration we will obtain velocities and positions of atoms. Through this various quantities of the system can be determined such as enthalpy, potential energy, kinetic energy, free energy, etc.

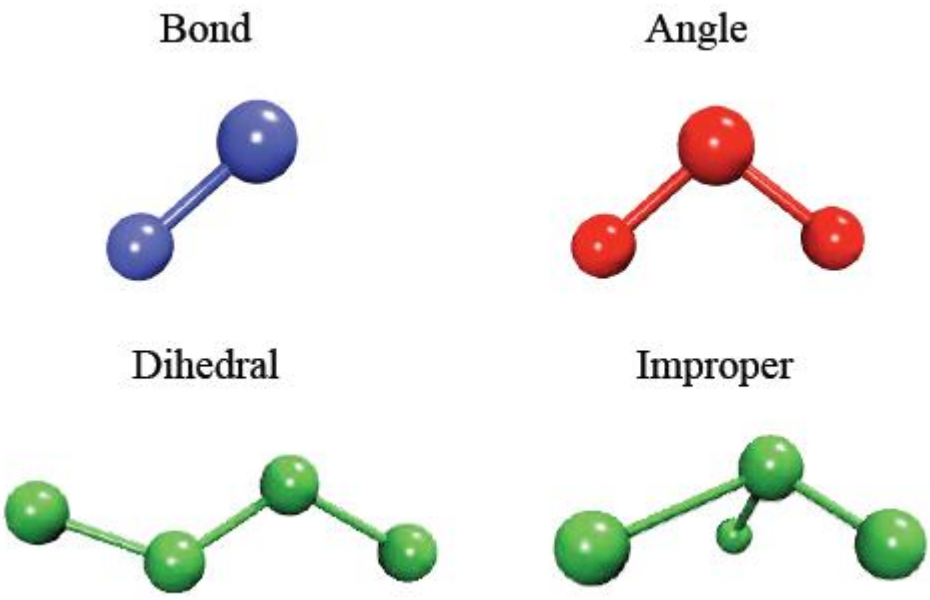

Figure 2.10: Other types of force field using in molecular structure [9].

There are also others simple force field that can be used to defined molecular structures that have been shown in Fig. 2.10. They can be combination of two types or more for more complex structures such as peptide and protein. However, in carbon nanostructure we only dealt with bonding potential that define the covalent bond between carbon atoms.

2.2.3 Prescribing Ensemble and Running Simulation

Before running an actual simulation, a thermalization process needs to be performed so that the system is at thermal equilibrium – which the system is at minimum energy. So, the ensemble is required to do this. To equilibrate the system, Microcanonical Ensemble (NVT) ensemble that using Nose-Hoover thermostat is mostly used [11]. The system is run at constant molarities, volume and temperature. It performs time integration on Nose-Hoover style non-Hamiltonian equations of motion which are designed to generate positions and velocities. This is achieved by adding some dynamic

variables which are coupled to the particle velocities (thermostatting). When used correctly, the time-averaged temperature of the particles will match the target values specified [12].

Next, simulation using Canonical Ensemble (NVE Ensemble) is run which means the system running at constant molarity, volume and energy. It performs integration to update the velocity and position for atoms in a system each timestep [13].

2.4. Thermal Transport in Carbon Nanostructure

In recent years, more and more electronic devices become smaller, the interface between the material properties on the overall thermal properties of materials more and more significant, especially when the small nanoscale materials, the interface thermal resistance will significantly affect the overall thermal conductivity of materials. Because carbon nanotubes and silicon [14] materials in thermal management are widely used in electronic devices, the study of the interface between these two thermal properties of materials becomes more and more important. This final year project uses the method of molecular dynamics simulations of carbon nanotube and graphene/graphite of its thermal conductivity was studied.

Table 2.1: Thermal conductivity of different carbon structures [15].

Sample	K (W/mK)	Method	Comments
Graphene	~3080 – 5300	Optical	Single layer
MW-CNT	> 3000	Electrical	Individual
SW-CNT	~ 3500	Electrical	Individual
SW-CNT	1750 – 5800	Thermocouples	Bundles
SW-CNT	> 3000	Thermocouples	Individuals
Graphite	~ 2000	Variety	In-plane
DLCH	~ 0.6 – 0.7	3-omega	H: ~20 – 35%
NCD	~ 16	3-omega	Grain size: 22 nm
UNCD	~6 – 17	3-omega	Grain size: < 26 nm
ta-C	3.5	3-omega	sp^3: ~ 90%
ta-C	1.4	3-omega	sp^3: ~ 60%
Diamond	800 - 2000	Laser flash	In-plane

Table 2.1 summarizes the thermal conductivities of graphene, single-wall carbon nanotubes (SWCNTs), multi-wall carbon nanotubes (MWCNTs), and bulk carbon materials and thin films. The data on NCD, UNCD, ta-C and hydrogenated diamond-like carbon (DLCH) is based on the experimental results. Recent study indicates that carbon nanotube has high thermal conductivity at room temperature [15], about ~3000W/mK. Furthermore, the thermal conductivity of nanotube can be further enhanced my adding a solid-solid interface such as silicon [16]. The length of tube and surface defect can also affect the thermal conductivity. Longer tube shown higher conductivity until it saturates at certain length.

Thermal conductivity of graphene is very hard to be determined through experiment [7]. Mostly it had been predicted through theoretical approach. The experiment performed by Alexander et al. [6] of graphene has thermal conductivity of

~4840 W/mK to ~5300 W/mK. It is higher compared to CNT. In simulation, several models have been tested to investigate the thermal conductivity of graphene and graphite. Nika et al. [17] determined the conductivity through phonon dispersion and they found the thermal conductivity is around 2000 W/mK to 5000 W/mK as the flake size increased (graphite). While Lan et al. determine the thermal conductivity through Green-Kubo function and they found K=3410 W/mK, just above conductivity of grapite compare to above situation. Baladin et al. [18] experiment also indicates that the thermal conductivity of single layer graphene is at ~4200 W/mK while graphite is at ~2000 W/mK. NEMD technique is applied to this simulation to find the thermal conductivity and is presented in this report.

2.4.1 Diffusion

Diffusion coefficient of a system can be obtained through mean-squared displacement of a group of atoms. Mean square displacement in the simulation system can be obtained by the following equation:

$$\text{MSD} = \langle |r(t) - r(0)|^2 \rangle \tag{2.7}$$

The amount of mean square displacement and diffusion coefficient of atoms there is a corresponding relationship. When the system is solid, that is, when the system temperature is below the melting point, there is the upper limit of the mean square displacement; and when the system is liquid, the mean square displacement is linear and its slope and there are atoms between the diffusion coefficient :

$$D = \lim_{t\to\infty} \frac{1}{6t} MSD \tag{2.8}$$

Experiment had been performed by Ruzicka et al. indicates that the diffusion at 3600K is 11000 $cm^2 s^{-1}$ through optical properties study [19]. Maasen el al. reported in

their experiment that they have diffusion coefficient of 20000 cm^2s^{-1} at room temperature through electron-hole mobility [20]. Simulation has also been performed by Lebedeva et al. [21] that graphene diffusion coefficient is 36000 cm^2s^{-1} at room temperature. The diffusion of graphite has yet been found in any literature and will be determined through molecular dynamics simulation.

2.4.2 Melting Transition

Phase transition is also a very interesting property to study in molecular dynamics. The phase transition, e.g. melting, can be determined by various methods. The conventional thermodynamics theory concludes that phase change would occur when there is a sudden change of energy and volume under a finite temperature and pressure. In molecular dynamics simulation, barostating is required to affect the phase change of the system, this will add a pressure terms to Nose-Hoover equation (NPT ensemble) which means constant molarity, pressure and temperature. Isobaric pressure is normally used to allow the volume change [21]. The simplest melting transition that can be observed is melting of FCC copper as shown in Fig 2.11 [22]. The different states of copper atom at different temperatures before melting occur also can be observed through Fig. 2.12.

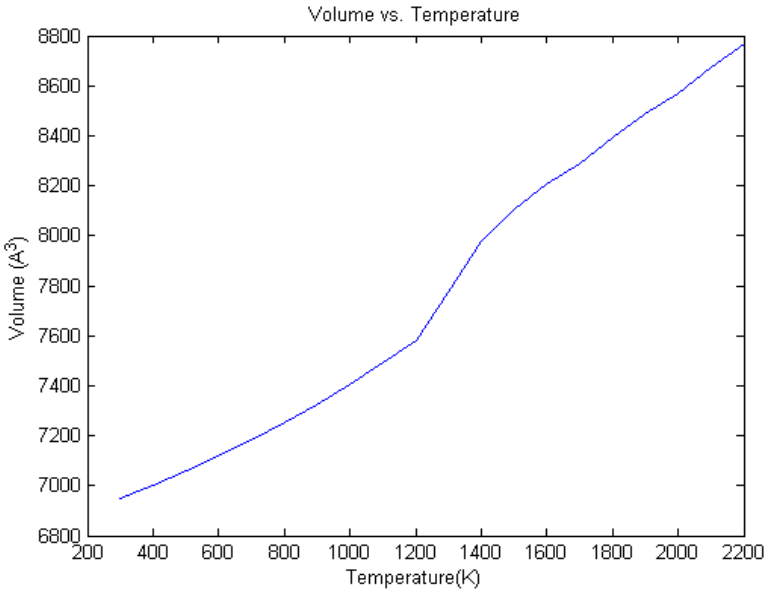

Figure 2.11: The sudden change of volume at ~1300 K indicates the melting point of copper. [22]

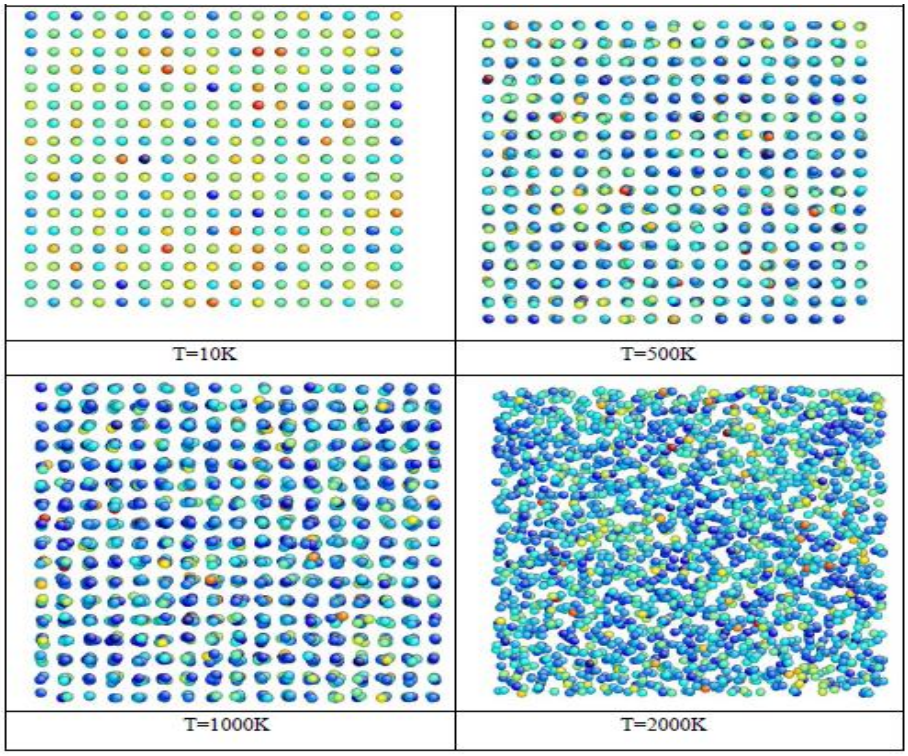

Figure 2.12: Different states of copper at different temperatures [22].

There are only limited literatures based on melting on graphene. However, the melting point of graphene has yet to be determined experimentally according to Geim [5]. A Monte-carlo simulation had been performed by Zakharzhenko et al. suggested that graphene melt at 4900K ~5200 K at zero pressure while graphite melts at 3000K~4250 K [23]. A simulation also performed by Ito et al. indicates that graphene melt at 5300 K ~ 5800 K [24]. Every literature reports that graphene has very high melting temperature.

2.4.3 Specific Heat Capacity

Specific heat capacity is derived from statistical mechanics. It defines total energy requires to heat up a quantity of substance by 1K. Several approaches had been conducted to determine the heat capacity of graphene and graphite either through experiment or simulation.

Zakharzhenko et al. suggested that graphene specific heat capacity at room temperature is ~24 $\mathrm{J\,mol^{-1}K^{-1}}$ [24] through Monte Carlo simulation. However the experiment has been conduct by Shafraniuk et al. indicates that the heat capacity is 8.5 $\mathrm{J\,mol^{-1}K^{-1}}$ [26]. While Yi et al. obtained the heat capacity through hot optical phonon and it's ~20 $\mathrm{J\,mol^{-1}K^{-1}}$ [27]. As the case of graphite, most literature agree that its heat capacity is around 0.6 $\mathrm{J\,mol^{-1}K^{-1}}$ ~ 0.9$\mathrm{J\,mol^{-1}K^{-1}}$. It can be summarized that the heat capacity of graphene do not agree with each other.

CHAPTER 3

SIMULATION METHODOLOGY

First, the training set of CNT has been investigated. Various force fields have been tested to find a stable structure of CNT when it is evolve at constant room temperature for a long timesteps. Then the stable CNT will be tested to see whether the physical properties are tally with the experimental results with the parameters that I have chosen.

Next, the thermal transport of is characterized using Non-equilibrium Molecular Dynamics (NEMD) simulations. The result obtained thus compared with the experimental result. The thermal gradient and total kinetic energy transfer is quantified to obtain the thermal conductivity.

Finally, all the tests will be involved in the transformation from graphene to graphite. Eventually, the thermodynamics properties will converge from graphene like properties to graphite like properties and the layers have been increased. The simulation is performed on single layer graphene to 7^{th}-layers of graphite.

3.1 Thermal Transport of Carbon Nanostructure

To validate the result from LAMMPS of thermal conductivity of (10, 10) armchair SWNT with diameter 1.375 nm at 300 K has been simulated using NVT ensemble. NEMD simulation has been implemented to get the temperature gradient resulting of swapping of kinetic energy.

$$J = -\lambda \Delta T \tag{3.1}$$

where ΔT is the gradient of the temperature, T, and J is the resulting heat flux. λ is the total kinetic energy transfer between slabs as denoted by

$$\lambda = \frac{\sum_{transfers} \frac{m}{2}(v_h^2 - v_c^2)}{2tL_xL_y < \partial T / \partial z >} \tag{3.2}$$

The subscripts *h* and *c* refer to the hot and the cold particle of identical mass *m* whose velocities are interchanged while *Lx* and *Ly* simulation box cross section area. The denominator 2 means heat flow in two directions of the slabs, effectively doubling the area of heat flux. The term $\partial T/\partial z$ is temperature gradient obtain from ensemble average.

Expression can be seen from the above, in order to find the thermal conductivity of the SWNT, this Muller Plathe method is used to apply heat [28] to the system as opposed to previous literature report on Green-Kubo method.

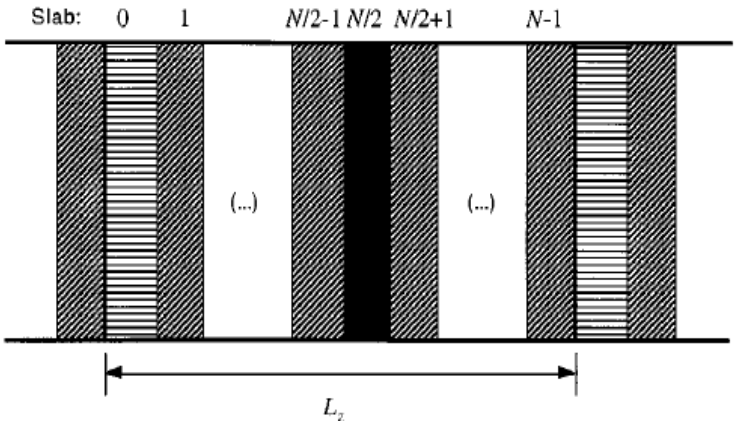

Figure 3.1: Muller-Plathe method, SWNT has been differentiated into several slabs.

The basic principle is shown in Fig. 3.1, the whole system is divided into slabs along the axial direction, and the temperature of each slab is calculated by the following statistics:

$$T_k = \frac{1}{3n_k k_B} \sum_{i \in k}^{n_k} m_i \upsilon_i^2 \tag{3.3}$$

Layer 0 is assumed as the cold slab, while layer N/2 is hot slab. The hottest atom (maximum kinetic energy) at cold slab exchange kinetic energy with the coldest atom (minimum kinetic energy) at hot slab. This will cause the temperature of hot slab increase and temperature at cold slab decrease, resulting in a heat flux between hot and cold slab. This happens because there is a temperature gradient between two atoms and distribution of kinetic energy of atom is very broad, therefore the hottest atom at cold slab always has greater kinetic energy than coldest atom at hot slab. The linear momentum and energy of the system is conserved if the mass of the swapping atoms remain the same. However, the angular momentums of the atoms are not conserved. This is not a problem because periodic boundary is introduced to the system; the angular momentum can be neglected.

The Muller-Plathe algorithm is relatively easy to implement, as well as keep the system linear momentum, the total kinetic energy and total energy conserved, and does not require an external heat bath, and it has been widely used. However, we note that Muller-Plathe method assumes that the cold slab and hot slab exchange of atomic mass are equal.

A simulation configuration of 10 nm × 10 nm × 49.12 nm simulation box that consist of (10, 10) armchair SWNT that build from 8000 carbon atoms, 1.375 nm diameter and 0.249 nm pore size as shown in Fig 3.2. Periodic boundary condition is implied to emulate “infinite space”. Another new emperical force field, namely AIREBO (Adaptive Intermolecular Reactive Empirical Bond Order) [29] will be implemented to the carbons.

$$E = \frac{1}{2}\sum_{i=1}^{N}\sum_{j\neq i}^{N}\left[E_{ij}^{REBO} + E_{ij}^{LJ} + \sum_{k\neq i,j}\sum_{l\neq i,j,k} E_{kijl}^{TORSION}\right]. \tag{3.4}$$

The REBO term is a functional form as hydrocarbon REBO potential for short range interaction. To compensate for the long range interaction to add accuracy to the force field, Lennard-Jones term had been added that same as conventional Lennard-

Jones potential and addition of torsion term that define four body potential that bonded at dihedral angle.

Then, the system will be equilibrated at 300K using NVT ensemble for 40000 timesteps (each steps is 1ps). After the system is equilibrating, heat flow is imposed to the system and run for two million timesteps in order to obtain the best temperature profile. Hence temperature gradient and total kinetic energy transferred can be calculated to obtain thermal conductivity of the system. Then, time averaging will be performed to obtain the mean squared displacement of the system. Plot the graph MSD versus time and the slope will represent the diffusion coefficient, *D*.

Method above will be applied almost the same in graphene and graphite system except the dimension of the simulation box is 3.93167 nm × 3.83054 nm × .6.0336 nm, 576 carbon atoms for graphene as shown in Fig. 3.3 and at subsequent layers the number of atom eventually multiply. The major objective of the simulation is to compare the thermal conductivity of graphene at different layers.

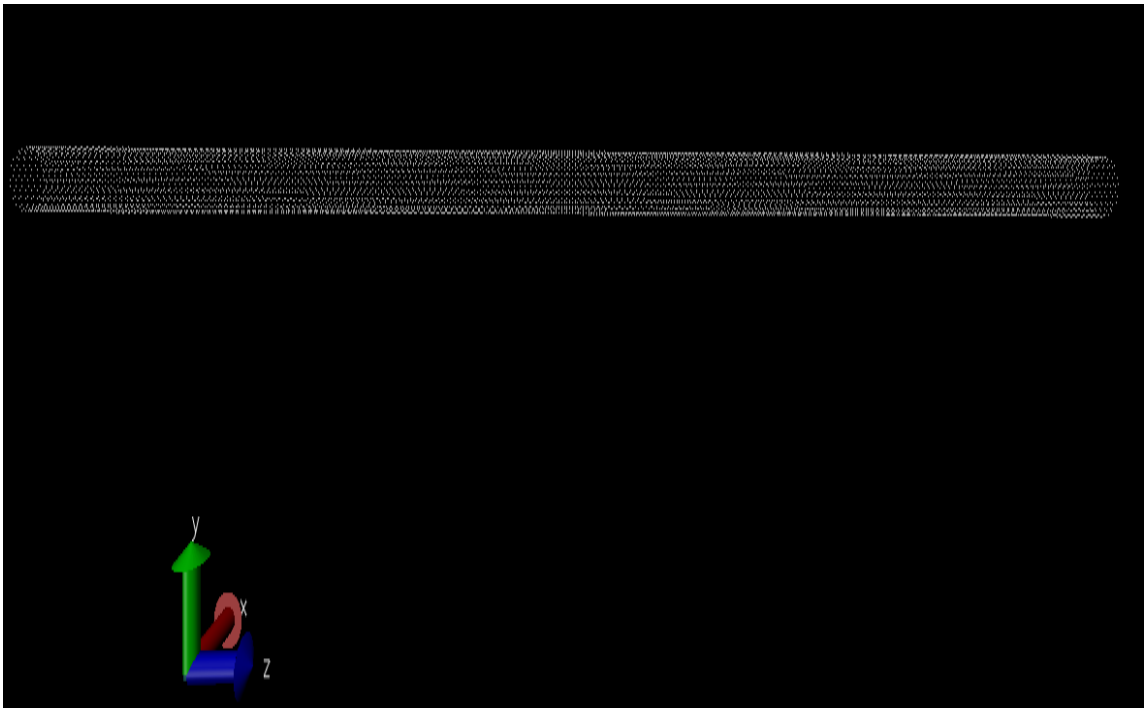

Figure 3.2: Initial condition of SWNT consists of 8000 carbon atoms.

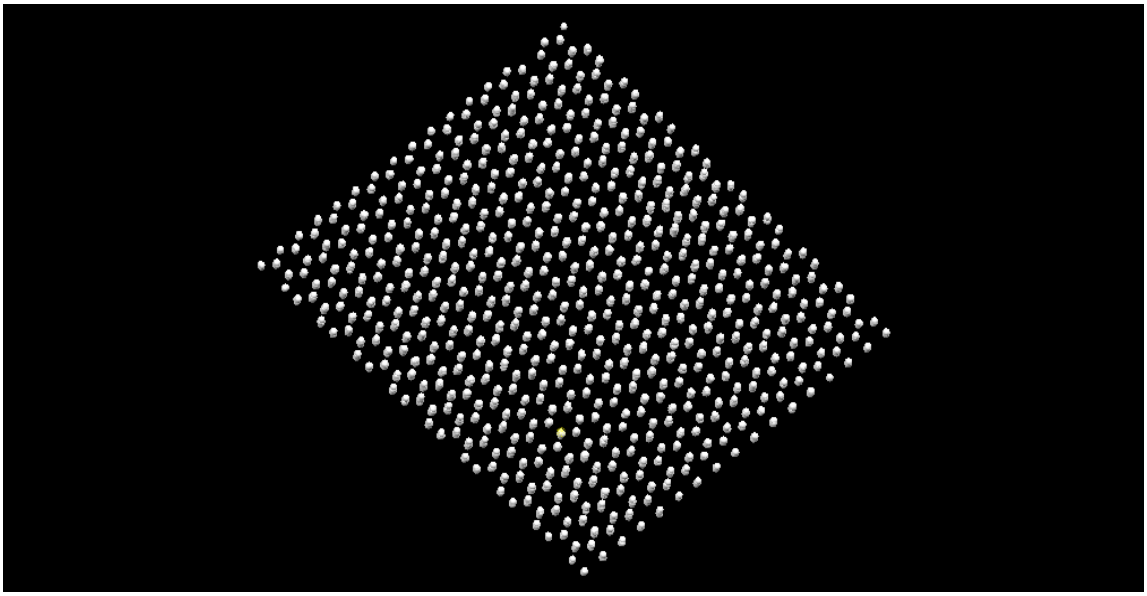

Figure 3.3: Initial condition of single layer graphene.

3.2 Melting and Specific Heat Capacity of Carbon Nanostructures

A simulation configuration of 3.93167nm × 3.83054nm × .6.0336nm consists of 576 carbon atoms for graphene and at subsequent layer the number of atoms eventually multiply and the pore size is 0.249 nm. Then, NVT ensemble is used to perform thermalization until the system reach equilibrium at 400000 timesteps (each timesteps is 1ps). After that, to induce volume change, thermostating and barostating is required, thus, NPT isobaric ensemble is used at atmospheric pressure 1 atm that run for four million timesteps.

Plot the graph volume or potential energy versus temperature, the sudden increase of volume or potential energy indicates that phase transition occur at that temperature. The snapshot of initial condition and melting of the graphene (and graphene) will be recorded. Then determine the melting temperature of different layer of graphene sheets is determined.

The information of specific heat capacity can be obtained via the log of equilibration of the first 400000 timesteps. The heat capacity equation is derived via statistical mechanics:

$$C_v = \frac{\partial E}{\partial T} \tag{3.5}$$

$$= \frac{<E_p^2> - <E_p>^2}{RT^2} \tag{3.6}$$

The heat capacity is calculated via fluctuation of the potential energy of the system. The variance of energy fluctuation is determined, R is universal gas constant and T is temperature. However, due to our system is very small (576 atoms to 4608 atoms), it is saved to say that it is preferable to use the equation difference of energy over the difference of temperature. The graph of energy versus temperature is plotted and the slope will determined the heat capacity. Next the heat capacity versus layer is examined.

CHAPTER 4

RESULTS AND DISCUSSIONS

4.1 Thermal Conductivity

The temperature profile, as shown in Fig. 4.1, is plot from energy versus layer of SWNT resulting of their kinetic energy are exchanged. The average slope of the graph will be temperature gradient.

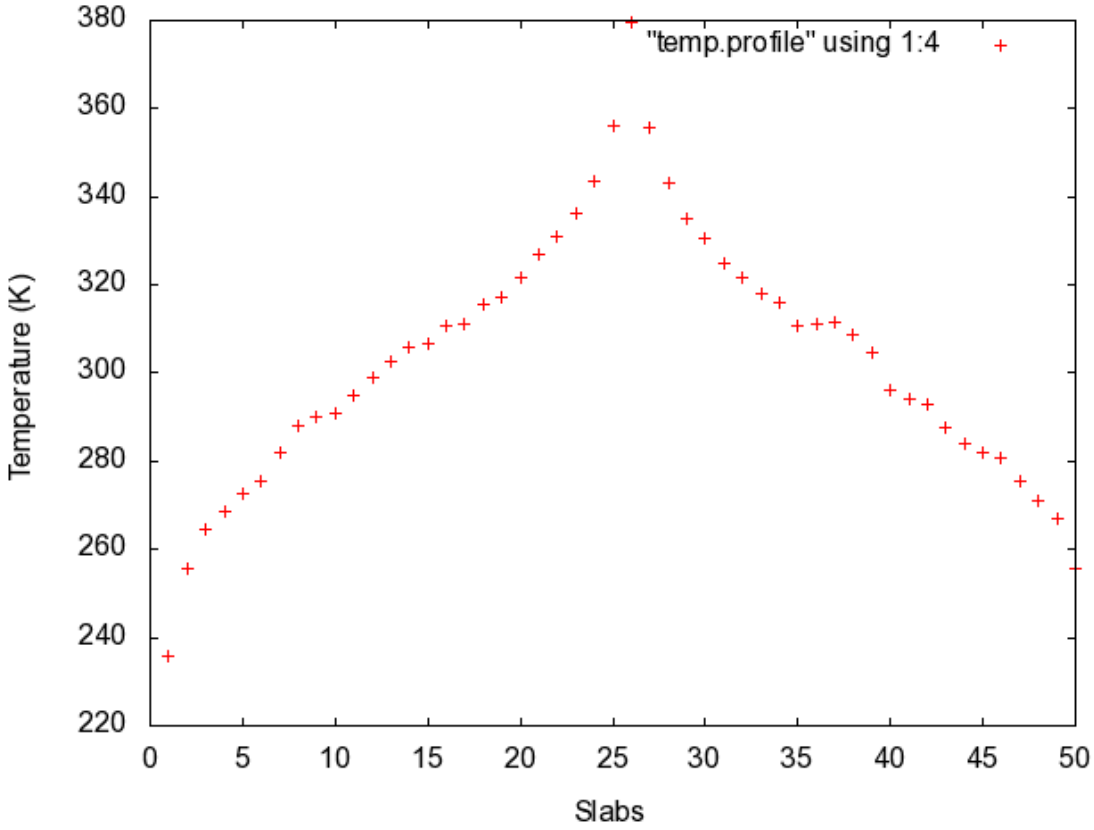

Figure 4.1: Temperature Profile of SWNT at 300K.

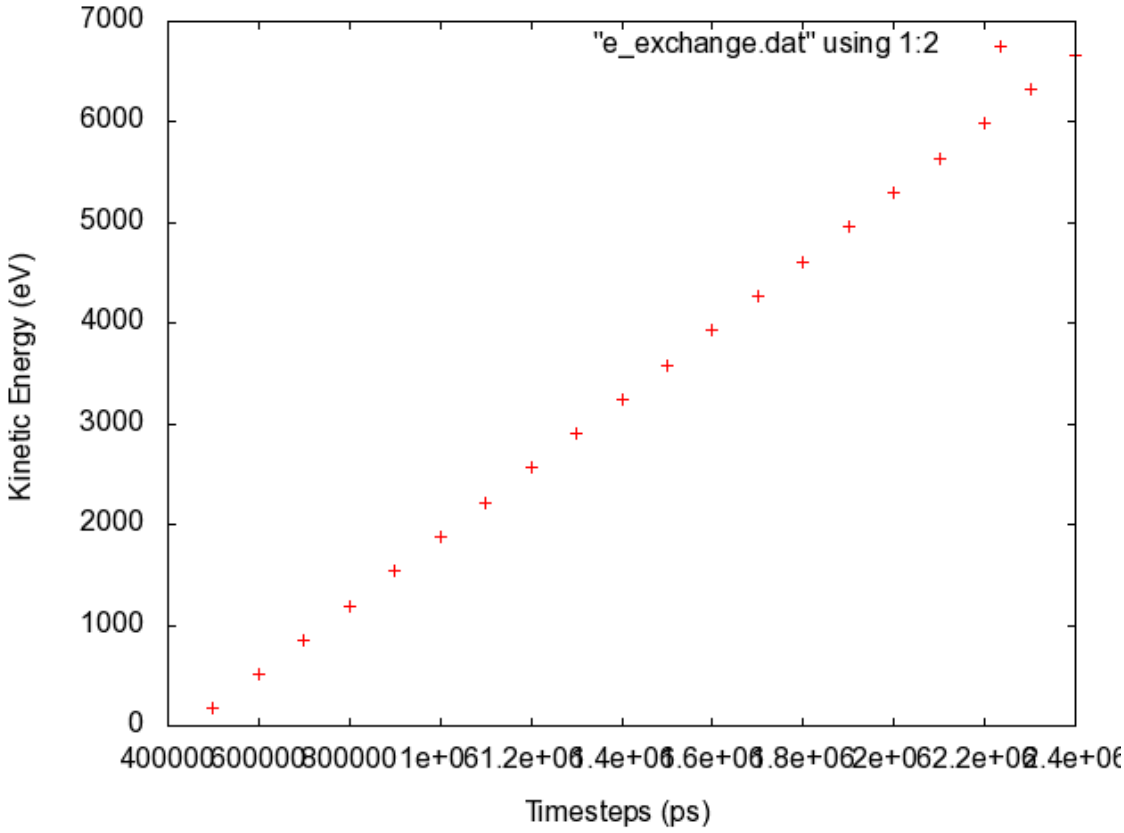

Figure 4.2: Cummulative kinetic energy swapped of SWNT.

The total kinetic energy that is transferred by these swaps that shown in Fig. 4.2 is then divided by time and the cross-sectional area of the simulation box yields a heat flux. The resulting heat flux is **J = 1.0679 × 10^-10 J/s.** The ratio of heat flux to the slope of the temperature profile is the thermal conductivity. The slope is obtained by performing linear fitting on the curve using GNUPLOT. The obtained slope is 0.37 K/Angstrom. So the thermal conductivity of SWNT is **2886.3 W/mK** as compared to experiment and other simulation model which the thermal conductivity yields around ~3000 W/mK to 3500 W/mK [15]. The thermal conductivity is at 5 % to 10 % tolerance compared with literature.

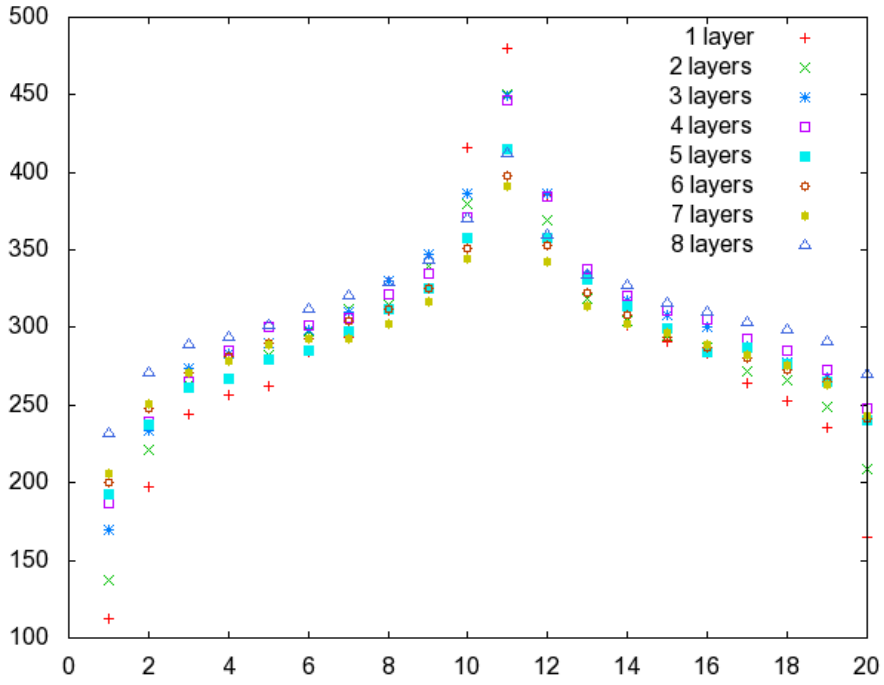

Figure 4.3: Different temperature profile of single layer graphene to 8th layer graphene.

As shown in Fig. 4.3, the temperature profiles for different layer of graphene are compared as well as their total kinetic energy swapped as shown in Fig 4.5.

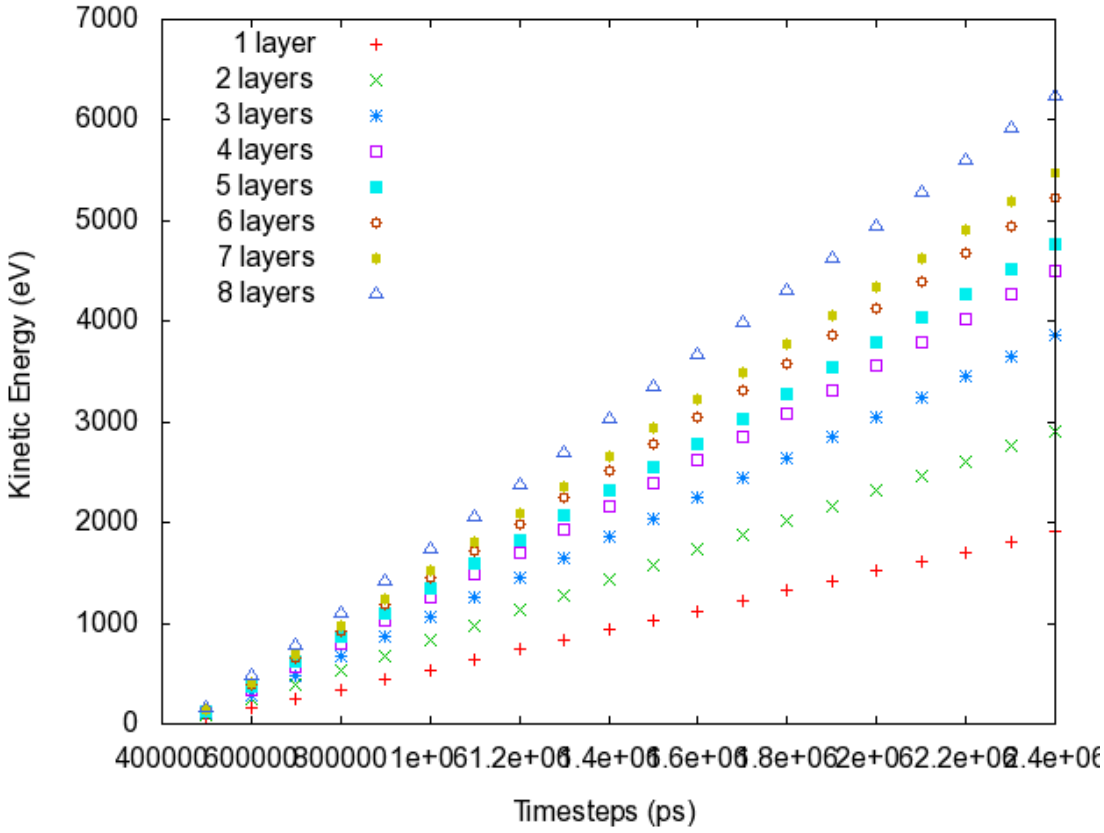

Figure 4.4: Cummmulative kinetic energy swapped of single layer graphene to 8th -layer graphene.

The way to obtain the thermal conductivity is similar to compute the thermal conductivity of SWNT using Muller-Plathe method through Eq. (3.2). The thermal conductivity of different graphene sheets will be displayed in Table 4.1 and Fig. 4.5.

Table 4.1: Thermal conductivity of different layer of graphene.

No. of Carbon Layer	Total Kinetic Energy (eV)	Thermal Conductivity (W/mK)
1	1905.2	4467.78
2	2912.66	3009.9
3	3858.17	2560.7
4	4504.8	2247.98
5	4773.31	1974.21
6	5225.14	1762.88
7	5477.36	1601.16
8	6244.97	1482.91

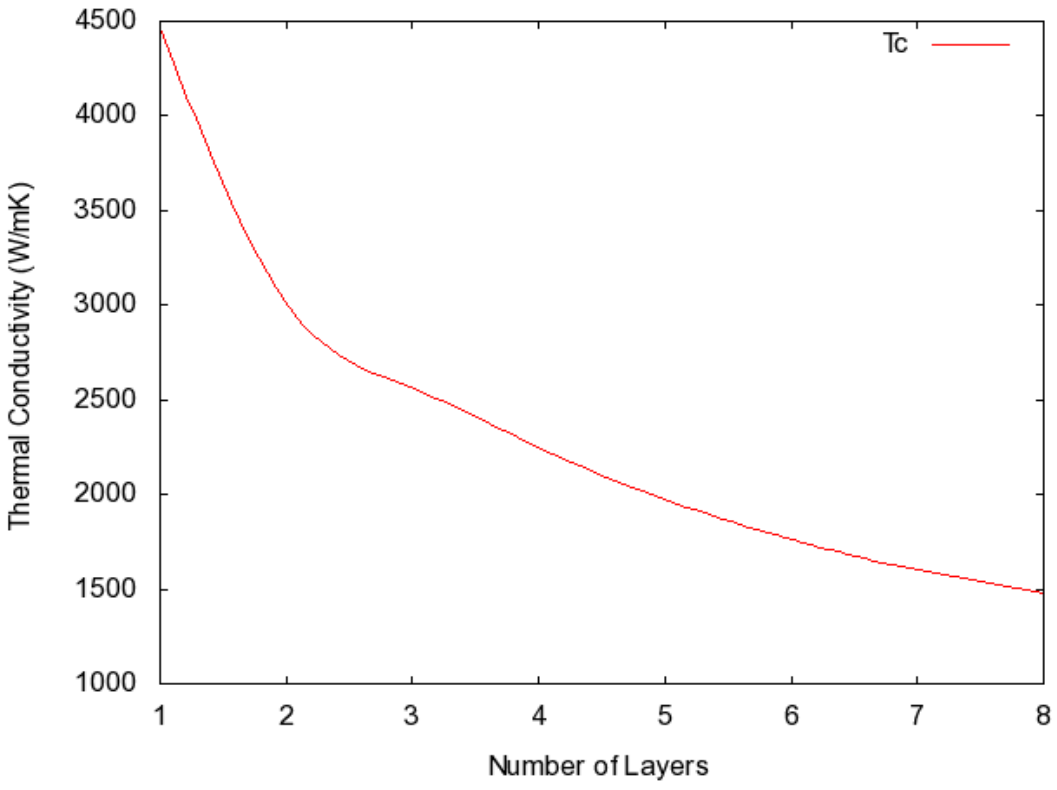

Figure 4.5: Thermal conductivity of graphene versus its layers.

As can be observed, carbon nanostructure possessed high thermal conductivity and the simulation results are comparable to theory and experiment. Low dimension nanostructure tends to have higher thermal conductivity than the higher dimension. The thermal conductivity in from single layer graphene to a few layers graphene varied from 4400 W/mK to 1480 W/mk, while for SWNT is at 2886.3 W/mk.

Thermal conductivity is induced by phonon scattering either by intrinsic phonon scattering or extrinsic phonon scattering. Intrinsic phonon scattering included phonon-phonon interaction (electron-phonon interaction is neglected due to limitation of molecular dynamics to take account of quantum effect). Carbon atoms in single layer graphene just interact with the atom at its own layer. The single layer graphene has ballistic transport, which means it requires minimal amount of energy to induce lattice vibration. The Umklapp process is happened during the phonon scattering – is a phonon created beyond Brillioun zone boundary. This can be further elaborated by the direction of heat transfer. In this case, the heat transfer occurred at direction of y-axis. The energy may disperse to other axis phonon scattering appeared. So this phenomenon will cause the reduction of thermal conductivity. However, the momentum and energy is difficult to conserve at low dimension during Umklapp process, this may suggest that 1-D SWNT has lower thermal conductivity compared to 2-D graphene.

4.2 Specific Heat Capacity

According to statistical mechanics, the information regarding specific heat capacity through random sampling of potential energy of the systemis obtained; hence the variance of potential energy of the system as the equation stated above (Eq. 3.6) need to be found.

As for the case of graphene, the same method will also be adopted to obtain its heat capacity. The heat capacity of graphene layers will be listed in Table 4.2 below:

Table 3.2: Heat capacity of graphene sheets.

No. of Carbon Layer	Heat Capacity (J $mol^{-1}K^{-1}$.)
1	~24.87
2	~17.68
3	~11.37
4	~6.66
5	~2.31
6	~1.14
7	~0.95
8	~0.83

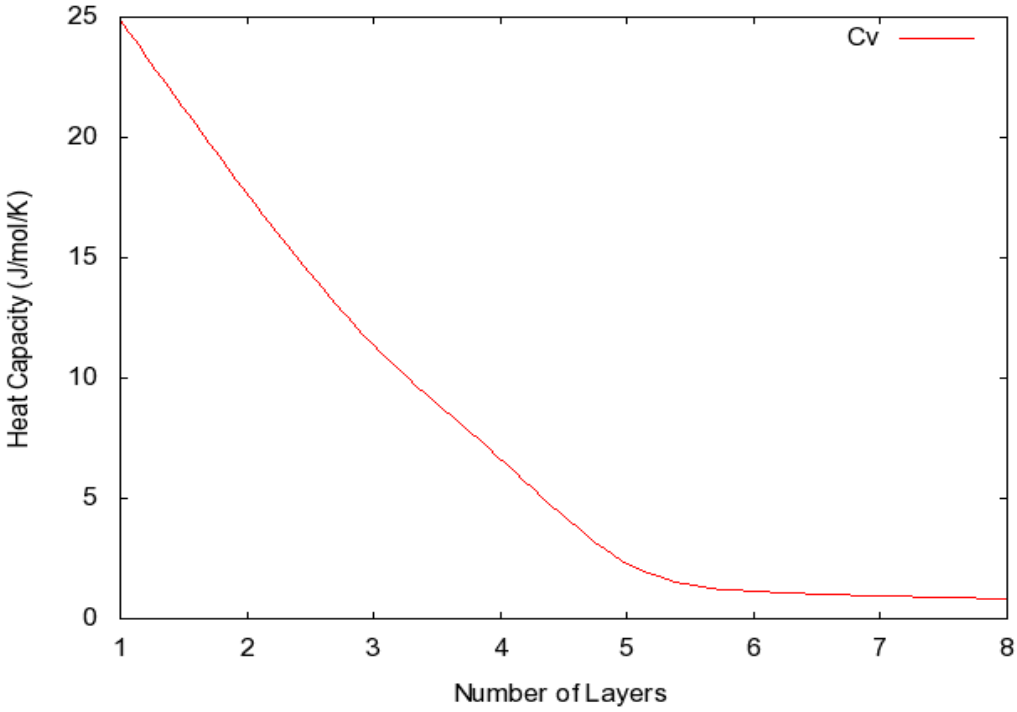

Figure 4.6: Heat capacity of graphene versus layers.

It can also been observed that the heat capacity decrease as the layer increase as shown in Fig 4.6. It can be assumed that it's because the mass of the system has been increased because heat capacity is inverse proportionally to mass. It also correlated with

thermal conductivity as the phonon scattering that carry the energy has been decrease but substitute by diffusion scattering. Their relation can be correlated with below equation:

$$K = \frac{1}{3} Cvl \tag{4.1}$$

The kinetic theory of gases provides a basic model for which thermal conductivity, *k*, depends on the specific heat, *C*, the velocity, *v*, (of the carrier of heat) and the mean free path, *l*.

So, more energy is required for the transport phenomena is bulk graphite because of the imperfection of the structure and energy is dispersed all around other axis.

4.3 Diffusion Coefficient

The amount of mean square displacement and diffusion coefficient of atoms has a corresponding relationship. When the system is solid, that is, when the system temperature is below the melting point, there is the upper limit of the mean square displacement; and when the system is in a liquid, a linear relationship between mean square displacements and timesteps will result with slope that define diffusion coefficient as shown in Table 4.3 and Fig. 4.7.

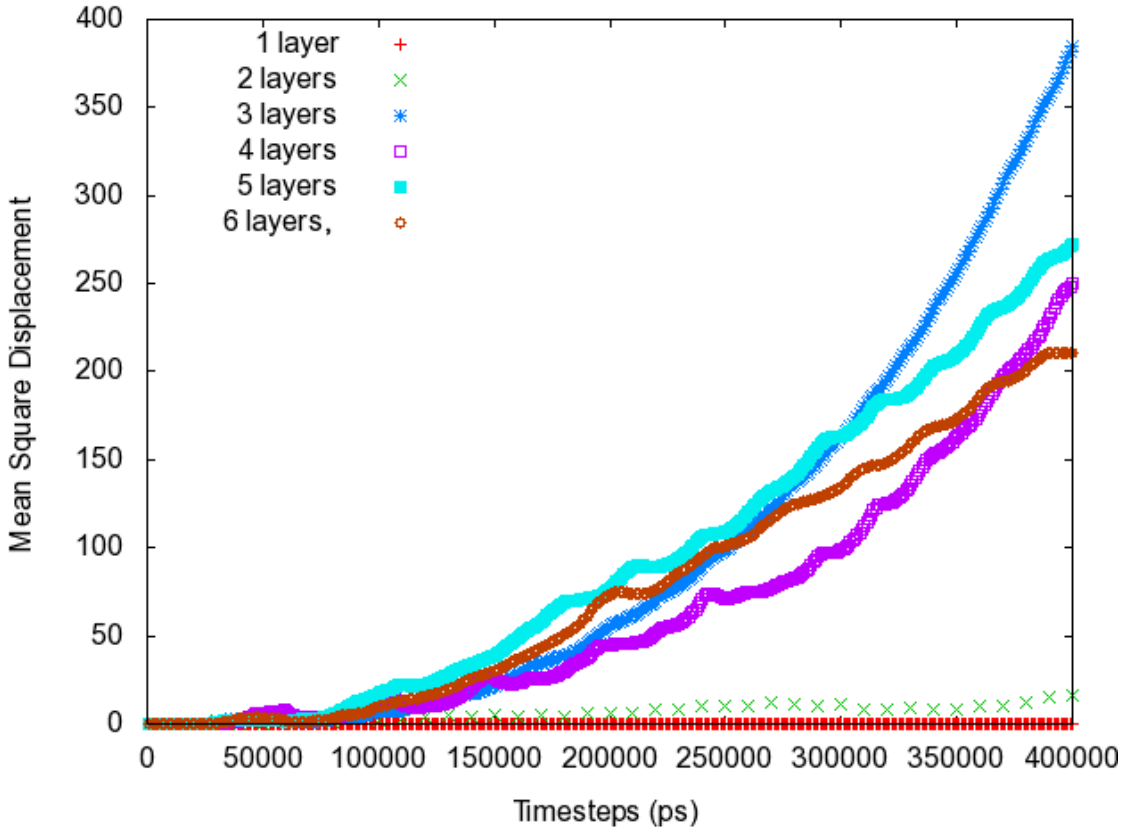

Figure 4.7: Diffussion coefficient of graphene sheets.

Table 4.3: Diffusion coefficient of graphene layers

No. of Carbon Layer	Diffusion Coefficient (cm^2s^{-1})
1	27.1456
2	64.68
3	233.5678
4	878.443
5	3132.31
6	10563.67
7	26025.5

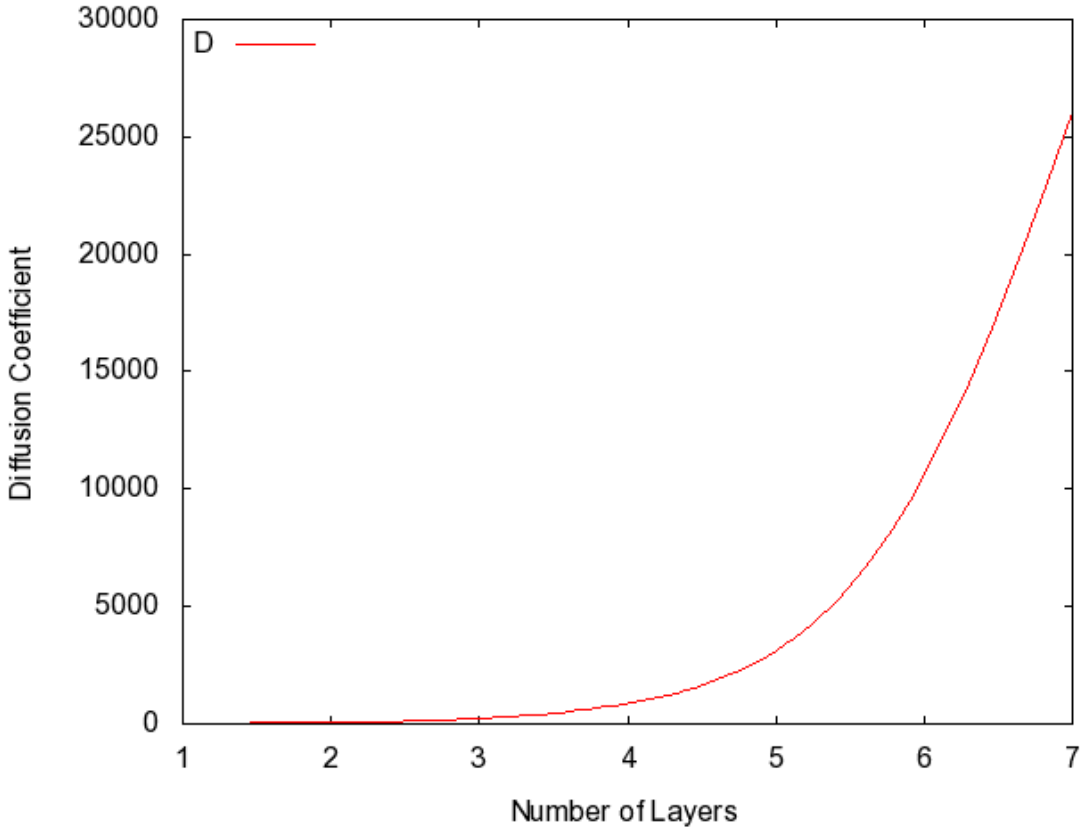

Figure 4.8: Diffusion coefficient versus layers of graphene.

The mean free path of phonon is limited by increasing the layers of grapheme as shown in Fig.4.8. This is because extrinsic factor such as structure defects, impurities and grain boundaries will limit the thermal conductivity of bulk structure. As the layer increase, diffuse scattering is more obvious than phonon scattering, thus, this has explained why diffusion coefficient increase with layers.

4.4 Phase Transition

To determine the phase transition, the melting transition in this case, the graph potential energy versus temperature has been plotted. A sudden rise of potential energy is expected during melting temperature. To further confirm the melting phase, volume versus temperature is plotted to compare with the result.

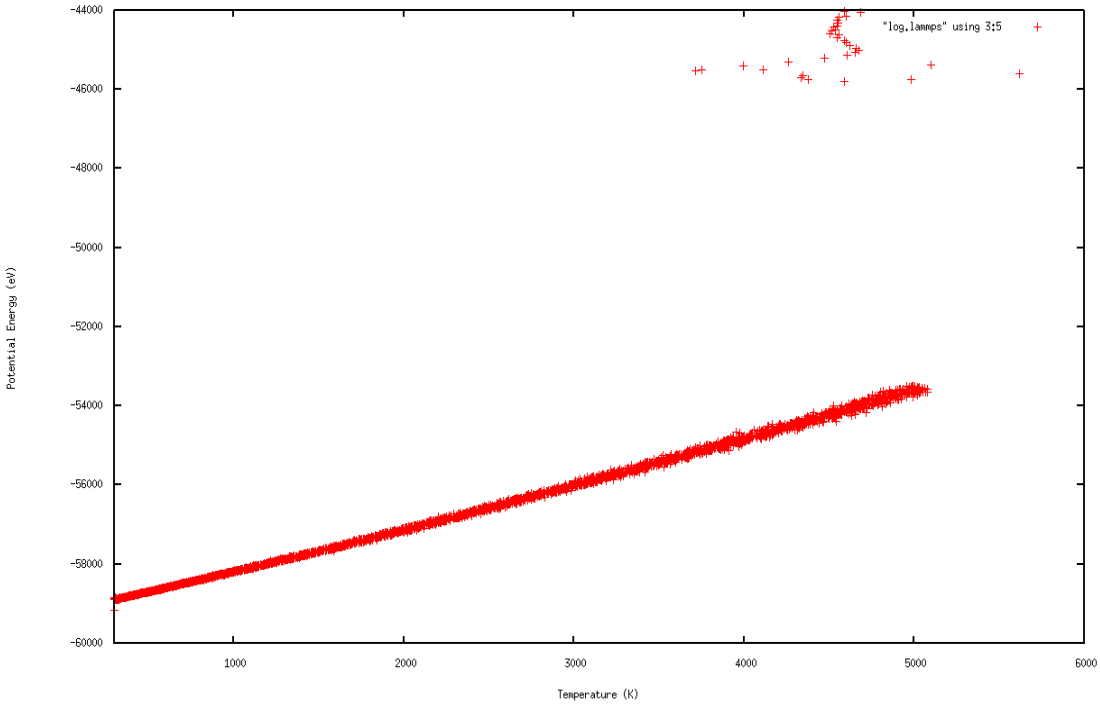

Figure 4.9: Graph of potential energy versus temperature of SWNT.

At solid form, as the temperature increase, the potential energy increased linearly too. As the SWNT reaching melting point, the potential energy suddenly shoots up at approximately 5045K. This graph suggested that the melting point of SWNT occurred during 5045K which it is at liquid phase as shown in Fig. 4.9.

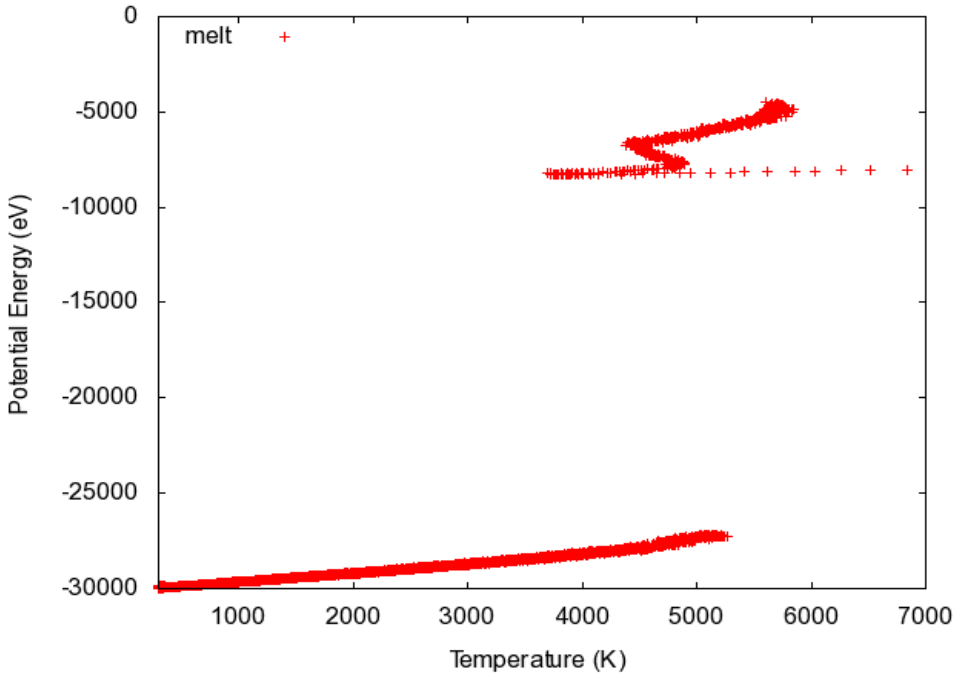

Figure 4.10: Melting phase of 7th layer of graphene by plotting potential energy versus temperature.

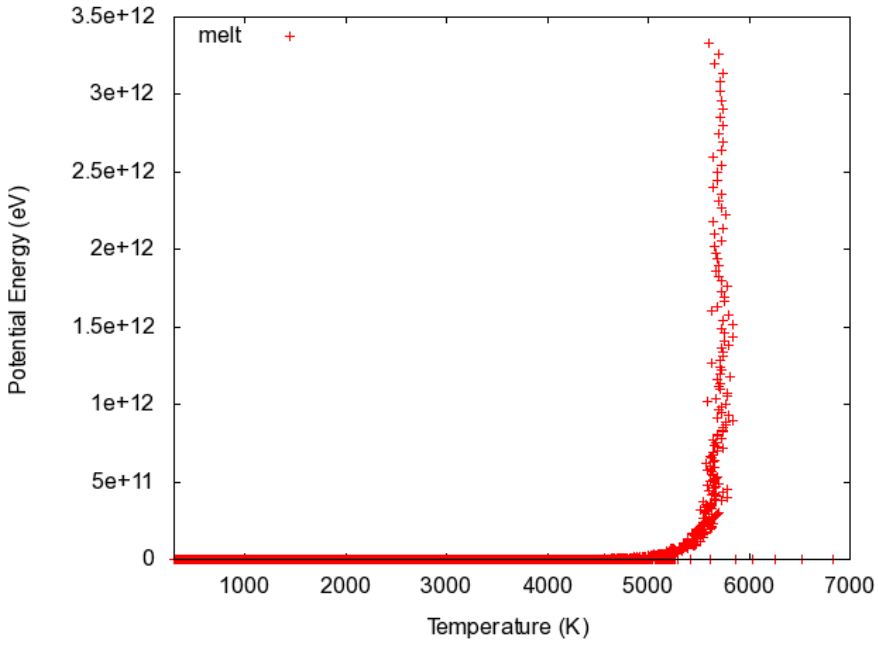

Figure: 4.11: Melting phase of 7th layer of graphene by plotting volume versus temperature.

As we can see, the melting of 7th layer of graphene occurs at approximately 5200 K according to Fig. 4.10. To further confirm the melting point, the plot of volume versus temperature can avoid the extraction of data regarding superheating as shown in Fig. 4.11.

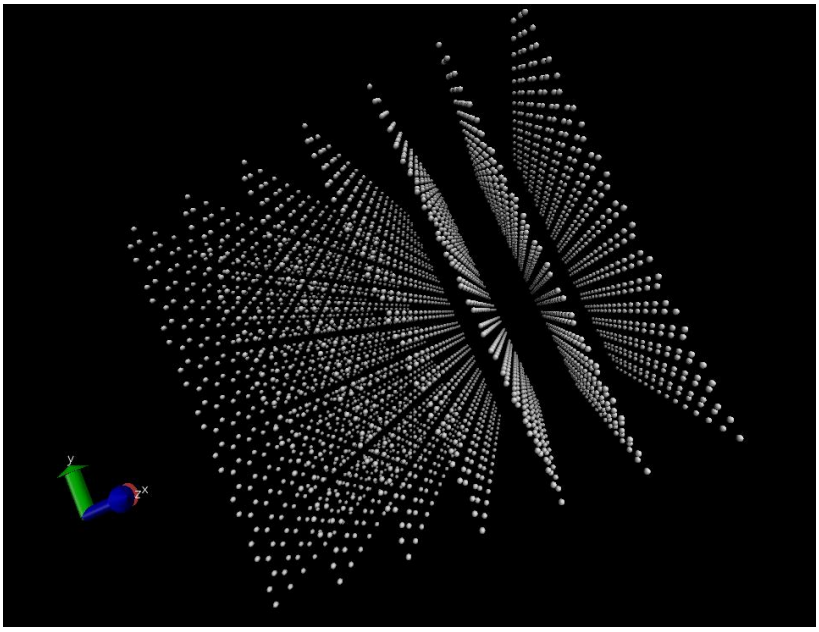

Figure 4.12: Initial configuration of 7th layer graphene at 300 K.

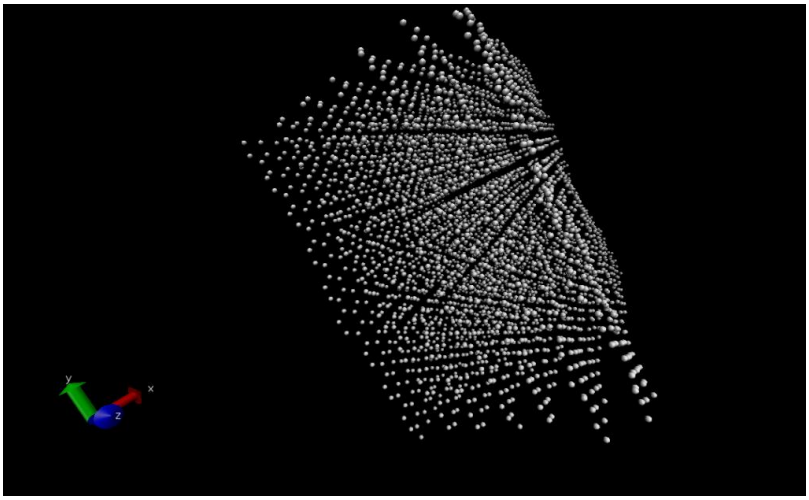

Figure 4.13: Configuration of 7th layer graphene at 1000 K.

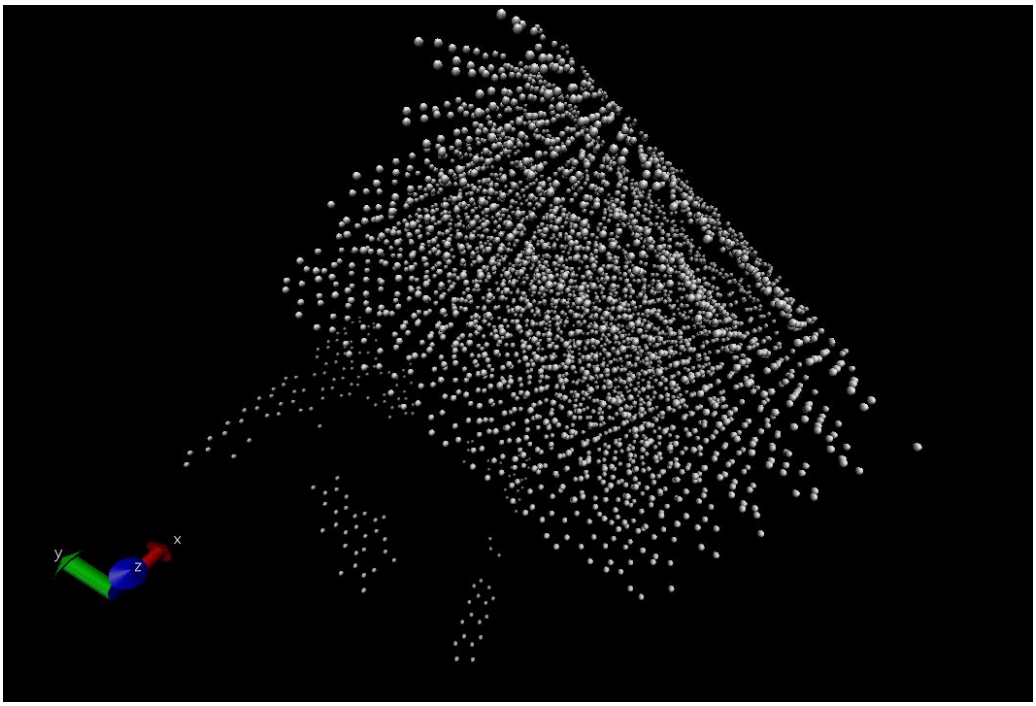

Figure 4.14: Configuration of 7th graphene at 3000 K.

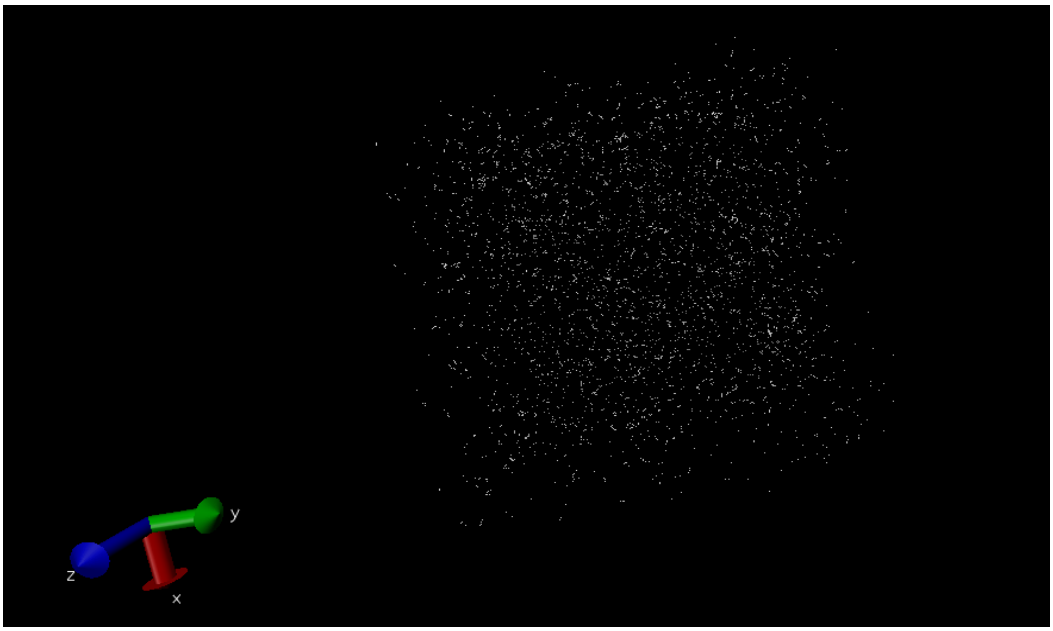

Figure 4.15: Configuration of 7th graphene at >5200 K (melting).

The status of the carbon atom at different temperature can also be monitored by using visualization tools such as VMD. The equilibrate structure at 300 K can be seen Fig. 4.12. To ensure the structure is equilibrated, the energy of the system has to be minimal. An to determine whether it is a stable layers of graphene, Van der Waals force has to be determined because by adding the subsequent layer, the Van der Waals force should be doubled as shown in Fig. 4.23. When the temperature has been increased to 1000 K as shown in Fig. 4.13, the carbon atoms in 7^{th} layers graphene begin to vibrate violently at its lattice. As the temperature keep increased to 3000 K as shown in Fig. 4.14, the carbon atoms vibrate more violently and some of its covalent bonds begin to break. As the temperature reaching melting point as shown in Fig. 4.15, the 7^{th} layer graphene has become liquid form and all covalent bond is completely broke and the lost its honeycomb shape as the carbon covalent bond that bond together seem "disintegrated".

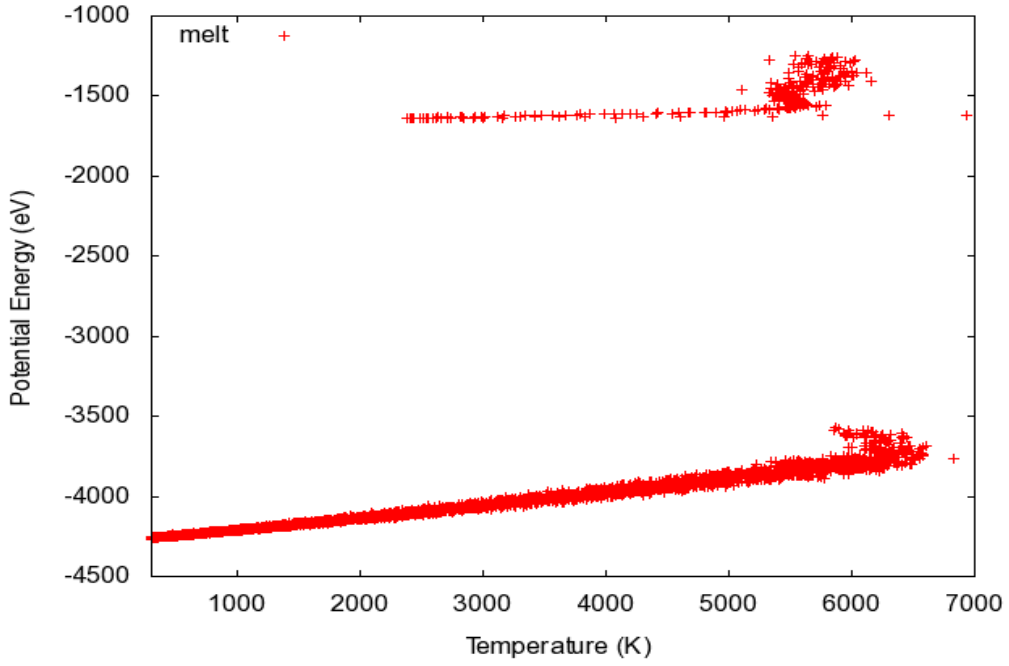

Figure 4.16: Phase transtion of single layer graphene by plotting potential energy versus temperature.

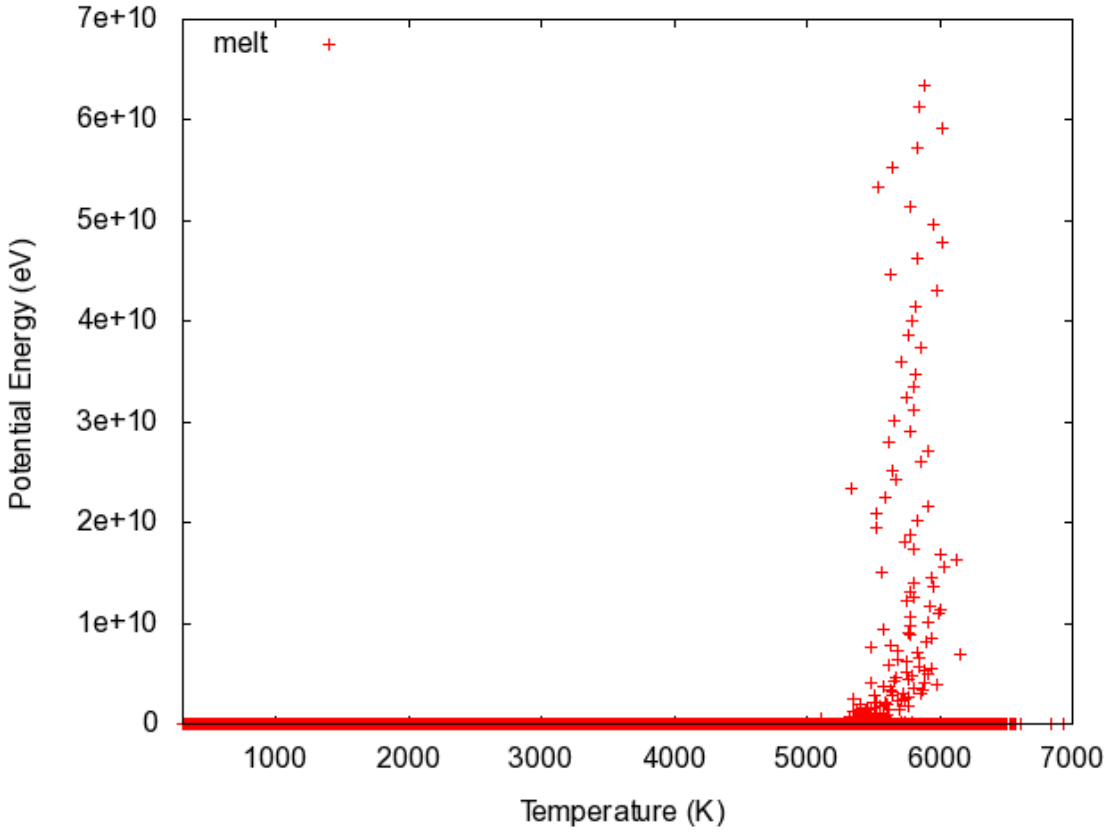

Figure 4.17: Phase transition of single layer graphene by plotting volume versus temperature.

As we can see, the melting of single layer graphene occurs at approximately 5350 K according to Fig. 4.16. To further confirm the melting point, the plot of volume versus temperature can avoid the extraction of data regarding superheating (in which will cause error during data extraction) as shown in Fig. 4.17.

.

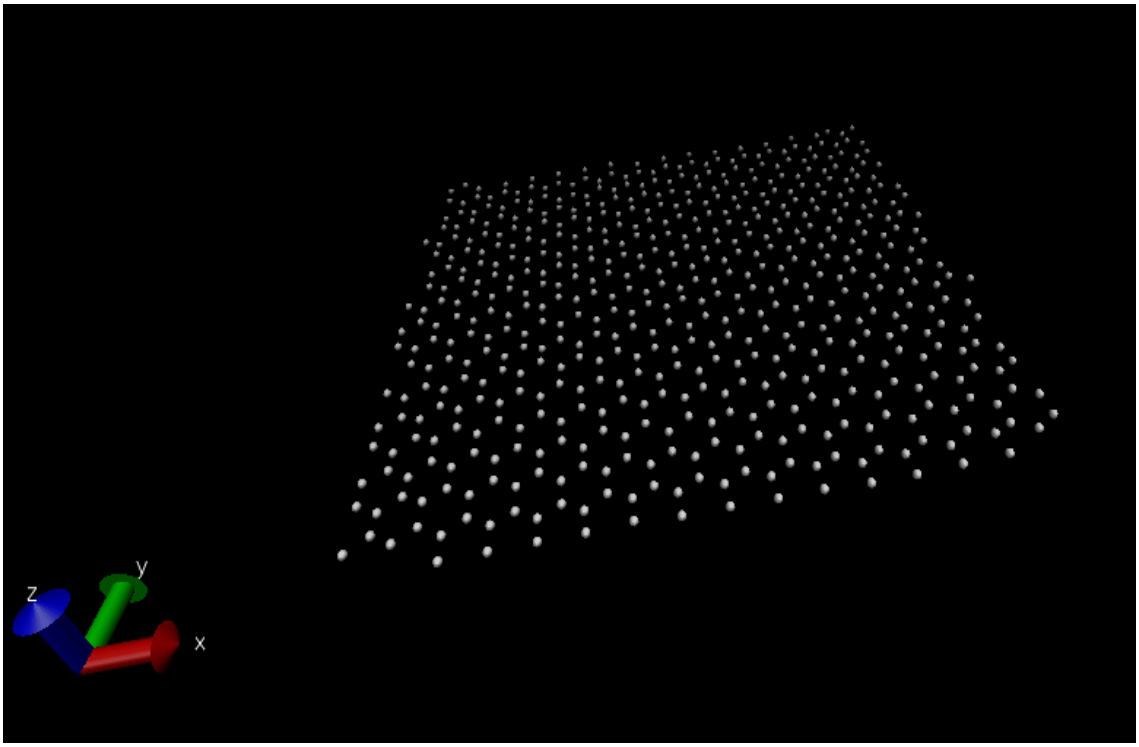

Figure 4.18: Configuration of single layer graphene at 300 K.

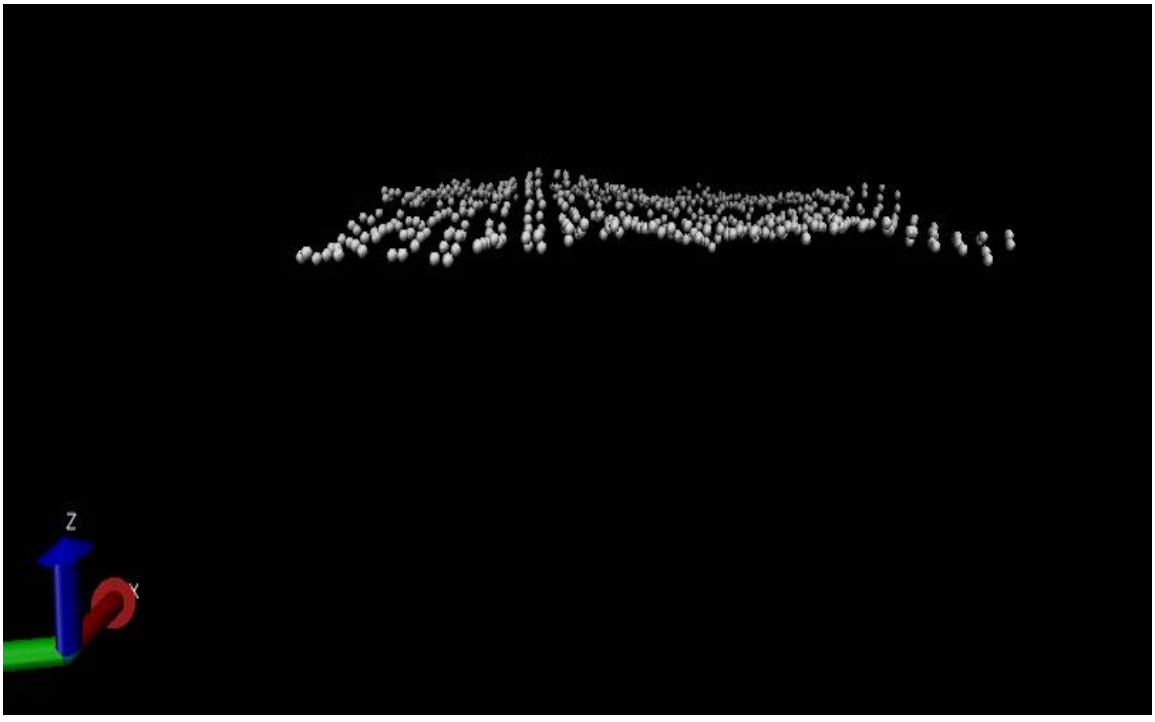

Figure 4.19: Configuration of single layer graphene at 1000 K.

Figure 4.20: Configuration of single layer graphene at 4000 K.

Figure 4.21: Configuration of single layer graphene at >5350 K (melting).

The equilibrate structure at 300 K can be seen Fig. 4.18. To ensure the structure is equilibrated, the energy of the system has to be minimal, or the fluctuation of pressure has to be also minimal. When the temperature has been increased to 1000 K as shown in Fig. 4.19, the carbon atoms in single layer graphene begin to vibrate violently at its lattice. As the temperature keep increased to 3000 K as shown in Fig. 4.20, the carbon atoms vibrate more violently and some of its covalent bonds begin to break. When the melting happened which shown in Fig. 4.21, the 2D grapheme layers melting into a 3D liquid network of 1D chain. Chain like carbon molecules are created when the covalent bond break loose.

Table 4.4: Relationship between melting temperature and number of layers.

No. of Carbon Layer	Melting Temperature (K)
1	~5350
2	~5320
3	~5300
4	~5270
5	~5245
6	~5220
7	~5200

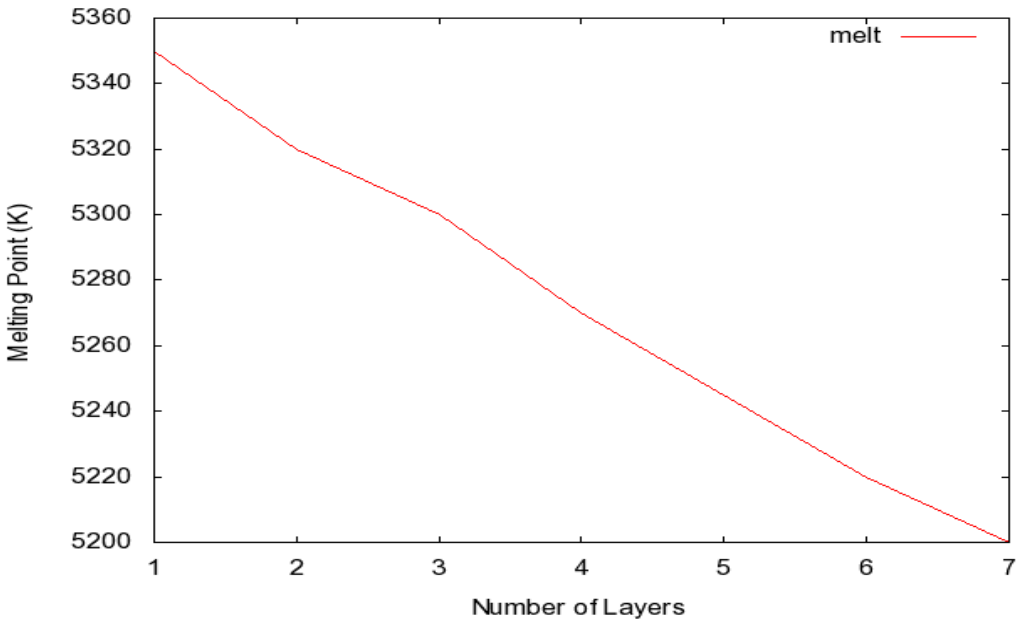

Figure 4.22: Melting temperature of graphene sheets versus its layers

Table 4.5: Relationship of cummulative Van der Waals force and number of carbon layers.

No. of Carbon Layer	Cumulative Van der Waals Force (eV/Angstrom)
1	~4250
2	~8520
3	~12780
4	~17070
5	~21300
6	~25580
7	~29800

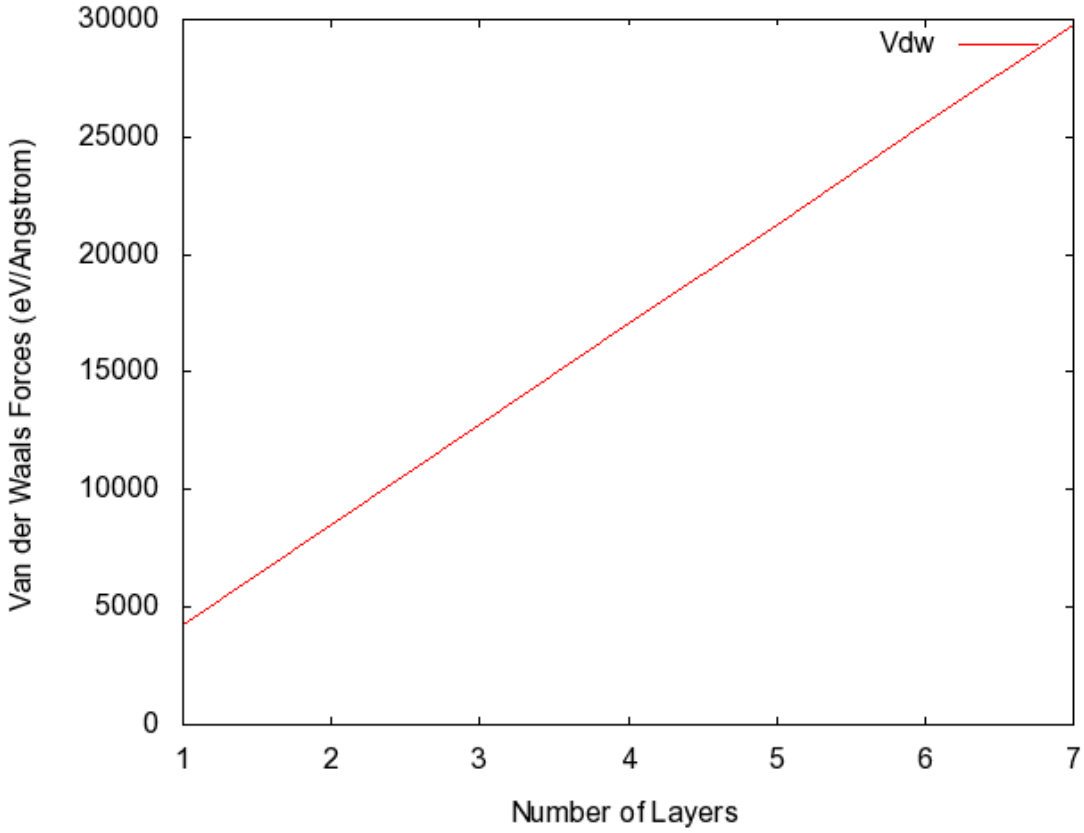

Figure 4.23: Cummulative Van der Waals forces versus number of graphene layers

Carbon nanostructures displayed high melting point. The melting temperature is slightly decreased as the increase with layer. This is because the carbon atom is bonded with a strong covalent bond to form a honeycomb shape. Overall, the melting point of graphene from graphite do not differ much, the difference is only by 3%. The 1-D structure of SWNT has lower melting point compared to 2-D graphene and 3-D graphite. The Van der Waals information shown in Table 4.5 and Fig 4.23 indicates whether the structure of each layer of graphene is stable or not. If the structure is stable, the the Van der Waals force will increase linearly with layers.

CHAPTER 5

CONCLUSIONS AND RECOMMENDATIONS

5.1 Conclusion

The study of thermal transport of carbon nanostructure has beed reviewed throughout its experiment and theoretical approach. Simulation has been performed to investigate the thermal transport properties of graphene and compared with with other carbon nanostructures, such as carbon nanotube and graphite. The thermal properties of graphene are superior campared to carbon nanotube and graphite because of the phonon interaction. It is very suitable to build many nanodevices that are beneficial to human such as heat sink at microprocessors because of its high thermal conductivity prospect.

The superior thermal properties of carbon nanostructures are fading as the dimension increased. However it is relatively easy to fabricate and cheap and still have its application in nanoelectronics. The high melting point is the only thermal properties that do not deviate much from graphene. So it is still appropriate to construct a high melting point carbon nanostructure by using graphite.

The molecular dynamics simulation maintains its accuracy at certain point. The data do not different much from experiment or other simulation results; the tolerance is within 5% to 10%.The physical properties of graphene do change with its number of layers.

5.2 Recommendation

Molecular Dynamics simulation requires skills of fine tuning. The inappropriate force field will result to the structure that not intended to obtain. Barostating and thermostating also need to be careful by tuning good damping parameters so the particles is relaxed enough before it increases its temperature or pressure. Timesteps

need to small enough so that the velocity and position of the particles can update more frequently for more accurate result.

Finding phase transition often have hysteresis curve resulting from superheating /super cooling beyond its phase change temperature. This error can be minimized by constructing 2 simulation box that for melting and solidification. Then, match the two graphs together to average the hysteresis error. For thermal conductivity computation, kinetic energy swapping cannot happen too frequently or else you may lose track to the temperature gradient.

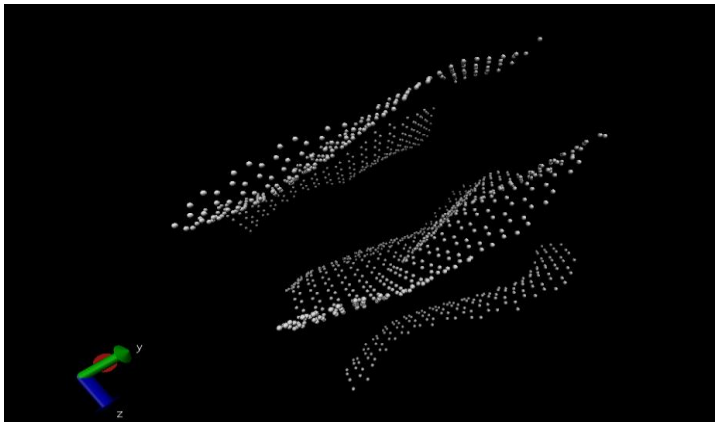

(a)

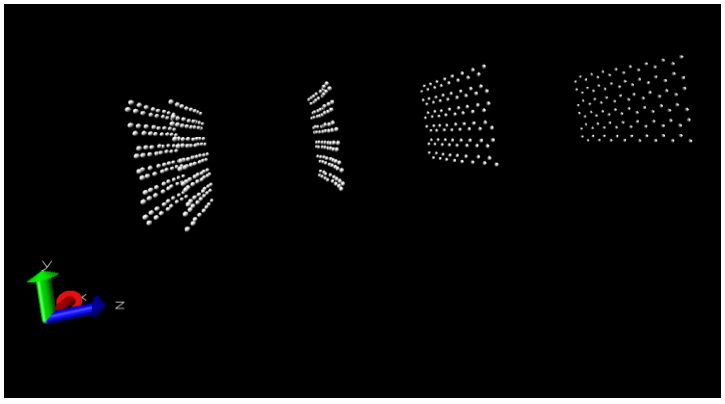

(b)

Figure 5.1: Inappropriate force field implementation results in wrong geometry in (a) and (b).

The computational resources are also very important. The program will run faster and efficiently in parallel computing rather than serial. MPI is implemented for parallel programming. The performance of MPI can even further enhanced by introducing OpenMP in to the system which is multithreading purposes. It reduces the communication times between computers. In future, GPU programming may be needed if the system is too complicated to increase the computational speed.

References

[1] J. Darabi. Micro- and nanoscale heat transfer: Challenges and opportunities. Heat Transfer Engineering, 23(2), pp. 1-2, 2002.

[2] G. Chen. Particularities of Heat Conduction in Nanostructures. Journal of Nanoparticle Research, 2(2), pp. 199-204, 2000.

[3] A. Rubio, D. Sanchez-Portal, E. Artacho, P. Ordejon, and J.M. Soler. Electronic States in a Finite Carbon Nanotube: A One-Dimensional Quantum Box. Physical Review Letter, 82(4), pp. 3520–3523, 1999.

[4] K. S. Novoselov, A. K. Geim, S. V. Morozov, D. Jiang, Y. Zhang, S. V. Dubonos, I. V. Grigorieva, and A. A. Firsov. Electric Field Effect in Atomically Thin Carbon Films. Science, 306(5696), pp. 666-669, 2004.

[5] C. Lee, X. Wei, J.W. Kyser, and J. Hone. Measurement of the Elastic Properties and Intrinsic Strength of Monolayer Graphene. Science, 321(5887), pp. 385-388, 2008.

[6] A. A. Balandin, S. Ghosh, W. Bao, I. Calizo, D. Teweldebrhan, F. Miao, and C. N. Lau. Superior Thermal Conductivity of Single Layer Graphene. Nanoletters, 8(3). pp. 902-907, 2008.

[7] A.K. Geim and K.S. Novoselov. The Rise of Graphene. Nature, 6(2) pp.183-191, 2007.

[8] Z. Sun, Z. Yan, J. Yao, E. Beitler, Y. Zhu, and J. M. Tour. Growth of Graphene from Solid Carbon Sources. Nature, 468(3). pp. 549-552, 2010.

[9] J. Thijssen (2007). Computaional Physics, Second Edition. United Kingdom: Cambridge University Press, pp. 197-252, 2007

[10] J. E. Jones. On the Determination of Molecular Fields. II. From the Equation of State of a Gas. Proceedings of the Royal Society of London. Series A, Containing Papers of a Mathematical and Physical Character, 106(738), pp. 463-477, 1924.

[11] S. Nose. A unified formulation of the constant temperature molecular dynamics methods. Journal of Chemical Physics, 81(5), pp. 511, 1984.

[12] A. Kohlmeyer and S. Plimpton. Lammps User Manual. USA: Sandia National Laboratary, pp. 385-386.

[13] S.Nose. A Molecular Dynamics Method for Simulation in Canonical Ensemble. Molecular Physics, 100(1), pp. 191 – 198, 2002.

[14] M.A. Angadi, T Watanabe, A. Bodapati, X.C. Xiao, O. Auciello, J.A. Carlisle, J.A. Eastman, P. Keblinski, P.K. Schelling, and S.R. Phillpot. Thermal transport and grain boundary conductance in ultrananocrystalline diamond thin film. Journal of Applied Physics, 99(11), pp.114301(1-6), 2006.

[15] M. A. Osman and D. Srivastava. Temperature dependence of the thermal conductivity of single-wall carbon nanotubes. Nanotechnology, 12(1), pp. 21-24, 2001.

[16] J. Diao, D. Srivastava, and M. Menon. Molecular dynamics simulations of carbon nanotube/silicon interfacial thermal conductance. Journal of Chemical Physics, 128(16), pp. 164708, 2008.

[17] D. L. Nika, E. P. Pokatilov, A. S. Askerov, and A. A. Balandin. Phonon thermal conduction in graphene: Role of Umklapp and edge roughness scattering. Physical Review, 79(2), pp. 155413 (1–12), 2009.

[18] J. Lan, J.S. Wang, C. K. Gan, and S. K. Chin. Edge effects on quantum thermal transport in graphene nanoribbons: Tight-binding calculations. Physical Review B, 79(5), pp. 115401 (1–5), 2009.

[19] B. A. Ruzicka, S. Wang, L. K. Werake, B. Weintrub, K. P. Loh, and H. Zhao. Hot Carrier Diffusion in Graphene. Physical Review B, 82(6), pp. 195414, 2010.

[20] J. Maassen, W. Ji, and H.Guo. Graphene spintronics: the role of ferromagnetic electrodes. Nanoletter, 11(1), pp. 151-155, 2010.

[21] I. V. Lebedeva, A. A. Knizhnik, A. M. Popov, O. V. Ershova, Y. E. Lozovik, and B. V. Potapkin. Fast Diffusion of Graphene Flake on a Graphene Layer. Physical Review B, 82(1), pp. 155460, 2010.

[22] M. Parrinello and M. Rahman. Crystal Structure and Pair Potentials: A Molecular Dynamics Study. Physical Review Letters, 45(2), pp. 1196-1199, 1980.

[23] O. H. Nielsen, J. P. Sethna, P. Stoltze, K. W. Jacobsen, and J. K. Norskov. Melting a Copper Cluster. Europhysics Letters, 26(1). pp. 51-56, 1994.

[24] K. V. Zakharchenko, J. H. Los, M. I. Katsnelson, and A. Fasolino. Atomistic simulations of structural and thermodynamics properties of bilayer graphene. Physical Review B, 81(1), pp. 235439, 2010.

[25] Y. Ito, M. Inoue, and K. Takashi. One-dimensionality of phonon transport in a cup stacked carbon nanofibers. Journal of Physics, 22(1), pp. 6, 2010.

[26] S. E. Shafraniuk and I. Kuljanishvili. Electric Energy Generation Arrays of Carbon Nanotube Junctions. Army Science Conference, 2009.

[27] K.S. Yi, D. Kim, and K.S. Park. Low energy electronic states and heat capacities in graphene strips. Physical Review B. 76(1), pp. 115410, 2010.

[28] Florian Muller-Plathe. Reversing the Perturbation in non-equilibrium molecular dynamics: an easy way to calculate the shear viscocity of fluid. Physical Review E, 59(1), pp. 4894-4898, 1999.

[29] D.W. Brenner, O.A Shenderova, J.A Harrison, S.J. Stuart, B. Ni, and S.B Sinnott. A second-generation reactive empirical bond order (REBO) potential energy expression for hydrocarbons. Journal of Physics: Condensed Matter, 14(4), pp. 783-802, 2002.

APPENDICES

Lammps input script to compute thermal conductivity of SWNT

```
# define the parameters of simulation and atoms
units           metal
dimension       3
boundary       p p p
atom_style      atomic
newton          on off

processors     * * 8

read_data       data.swnt

region            up    block  INF INF  INF INF  -0.614012  9.21018044  units
box
region            down  block  INF INF  INF INF   244.990799  254.81499144
units box


pair_style  airebo/omp 3.0 1 1

pair_coeff * * CH.airebo C

neighbor        4.0 bin
neigh_modify    delay 0 every 1 check yes

timestep        0.0005

velocity all create 300.0 31654 mom yes rot yes dist gaussian units box

# take some potential energy out of the system
minimize 1.0e-8 1.0e-6 1000 10000

reset_timestep 0

#fix     integrate   all nve
fix     thermostat  all nvt temp 300.0 300.0 0.1

# temperature is based on all atoms
compute alltemp all temp
thermo_style    custom step atoms temp press pe ke etotal xlo xhi ylo yhi zlo
zhi vol
thermo_modify   temp alltemp lost warn

#perform time-averaging to obtain temperature gradient
compute           ke  all  ke/atom
variable          temp atom  c_ke/(1.5*1.0)/8.617343*100000.0
fix               temp_profile    all    ave/spatial  1  100000  100000  z  -
0.614012 9.82419244  v_temp  file  temp.profile    units  box
fix               temp_atom    all    ave/atom  1  100000  100000 v_temp
compute           up_temp    all  temp/region up
compute           down_temp  all  temp/region down
variable          delta_t   equal  c_down_temp-c_up_temp
```

```
fix               delta_t  all  ave/time  1  100000  100000  v_delta_t   file
delta_t.dat
dump 1 all xyz 100000 dump.coord.*
dump 2 all custom 100000 dump.vel.* id type mass vx vy vz fx fy fz f_temp_atom

#calculate total kinetic energy
fix ensemble all nve
fix               heat_swap   all  thermal/conductivity  40  z  50
fix               e_exchange  all  ave/time  40  2500  100000  f_heat_swap
file  e_exchange.dat
variable          thermal_condt equal
f_heat_swap/(2.0*19.22808084*3.1415926*f_delta_t*(step-400000)*0.0005+1e-
10)*1.602*1.0e4

fix               thermal_condt  all  ave/time  100000  1   100000
v_thermal_condt   file  thermal_condt.dat

run               2000000
```

LAMMPS data files for the initial configuration of SWNT

```
8000 atoms
 0 bonds
 0 angles
 0 dihedrals
 0 impropers
 1 atom types
 0 bond types
 0 angle types
 0 dihedral types
 0 improper types
 -50.000000 50.000000  xlo xhi
 -50.000000 50.000000  ylo yhi
 -0.614012  490.59561  zlo zhi

 Masses

 1 12.010700 # CA

 Atoms

1 1 6.770451 0.000000 0.000000 # CA
2 1 6.622501 1.407656 0.000000 # CA
3 1 6.439082 2.092185 1.228024 # CA
4 1 5.863383 3.385226 1.228024 # CA
5 1 5.477410 3.979571 0.000000 # CA
6 1 4.530316 5.031426 0.000000 # CA
7 1 3.979571 5.477410 1.228024 # CA
8 1 2.753791 6.185115 1.228024 # CA
9 1 2.092185 6.439082 0.000000 # CA
10 1 0.707705 6.733362 0.000000 # CA
11 1 0.000000 6.770451 1.228024 # CA
12 1 -1.407656 6.622501 1.228024 # CA
13 1 -2.092185 6.439082 0.000000 # CA
14 1 -3.385226 5.863383 0.000000 # CA
15 1 -3.979571 5.477410 1.228024 # CA
16 1 -5.031426 4.530316 1.228024 # CA
17 1 -5.477410 3.979571 0.000000 # CA
18 1 -6.185115 2.753791 0.000000 # CA
19 1 -6.439082 2.092185 1.228024 # CA
20 1 -6.733362 0.707705 1.228024 # CA
21 1 -6.770451 0.000000 0.000000 # CA
22 1 -6.622501 -1.407656 0.000000 # CA
23 1 -6.439082 -2.092185 1.228024 # CA
24 1 -5.863383 -3.385226 1.228024 # CA
25 1 -5.477410 -3.979571 0.000000 # CA
26 1 -4.530316 -5.031426 0.000000 # CA
27 1 -3.979571 -5.477410 1.228024 # CA
28 1 -2.753791 -6.185115 1.228024 # CA
```

```
29 1 -2.092185 -6.439082 0.000000 # CA
30 1 -0.707705 -6.733362 0.000000 # CA
31 1 -0.000000 -6.770451 1.228024 # CA
32 1 1.407656 -6.622501 1.228024 # CA
33 1 2.092185 -6.439082 0.000000 # CA
34 1 3.385226 -5.863383 0.000000 # CA
35 1 3.979571 -5.477410 1.228024 # CA
36 1 5.031426 -4.530316 1.228024 # CA
.....................................................................................
```

LAMMPS input script for compute melting, diffusion coefficient and heat capacity

```
imension 3
boundary  p p p
units metal

atom_style atomic
processors * 3 4
read_data  data.lammps

#region            up    block  0.0000 1.9153  INF INF  INF  INF  units box
#region            down  block  19.1523 21.068 INF INF  INF  INF  units box
thermo_style    custom step atoms temp press pe ke etotal vol enthalpy
thermo 1000
pair_style  airebo/omp 3.0 1 1
pair_coeff * *  CH.airebo  C


replicate 1 1 5

neighbor        4.0 bin
neigh_modify    delay 0 every 1 check yes


timestep 0.00005


velocity all create 300 1234567 dist gaussian units box

fix     1  all nvt temp 300.0 300.0 1.0 drag 0.2
compute 1 all pe/atom
compute 2 all ke/atom
compute 3 all coord/atom 3.0
compute 4 all msd com yes
variable msdx equal "c_4[1]"
variable msdy equal "c_4[2]"
variable msdz equal "c_4[3]"
variable total equal "c_4[4]"
variable timestep equal "step"
fix 2 all ave/time 100 5 1000 c_4[1] c_4[2] c_4[3] c_4[4] file tmp.avetime
#fix 3 all print 10 "${timestep} ${msdx} ${msdy} ${msdz} {msdtot}" & screen no
file tmp.print & title "#Mean Square Displacement\n #x y z total"

dump 1 all xyz 10000 abc.xyz
dump 2 all custom 10000 dump.atom id c_1 c_2 c_3
```

```
compute 5 all rdf 50
fix 4 all ave/time 100 5 1000 c_5 file tmp.rdf mode vector

run 400000

unfix 1

fix 5 all npt temp 300.0 7000.0 1.0 iso 0.0 0.0 1.0 drag 0.2
dump 3 all xyz 10000 def.xyz
compute 6 all rdf 50
fix 6 all ave/time 100 5 1000 c_5 file melting.rdf mode vector

run 4000000
```

LAMMPS data files for initial configuration of graphene

```
76 atoms

1 atom types

0.0 39.316736 xlo xhi
0.0 38.305449 ylo yhi
0.0 6.704 zlo zhi

Masses

  1 12.01

Atoms

1      1      0.0000 0.0000 1.6760
2      1      0.0000 1.4186 1.6760
3      1      0.0000 4.2562 1.6760
4      1      0.0000 5.6747 1.6760
5      1      0.0000 8.5123 1.6760
6      1      0.0000 9.9309 1.6760
7      1      0.0000 12.7685 1.6760
8      1      0.0000 14.1871 1.6760
9      1      0.0000 17.0246 1.6760
10     1      0.0000 18.4432 1.6760
11     1      0.0000 21.2808 1.6760
12     1      0.0000 22.6994 1.6760
13     1      0.0000 25.5370 1.6760
14     1      0.0000 26.9555 1.6760
15     1      0.0000 29.7931 1.6760
16     1      0.0000 31.2117 1.6760
17     1      0.0000 34.0493 1.6760
18     1      0.0000 35.4679 1.6760
19     1      1.2286 3.5467 1.6760
20     1      1.2286 2.1281 1.6760
21     1      1.2286 7.8028 1.6760
22     1      1.2286 6.3842 1.6760
```

……